

Persistent coding of outcome-predictive cue features in the rat nucleus accumbens.

Authors: Jimmie M. Gmaz¹, James E. Carmichael¹, Matthijs A. A. van der Meer^{1*}

¹Department of Psychological and Brain Sciences, Dartmouth College, Hanover NH 03755

*Correspondence should be addressed to MvdM, Department of Psychological and Brain Sciences, Dartmouth College, 3 Maynard St, Hanover, NH 03755. E-mail: mvdm@dartmouth.edu.

Number of Figures: 12

Number of Tables: 1

Total Word Count: ?

Abstract Word Count: 150

Introduction Word Count: ?

Discussion Word Count: ?

Acknowledgments: We thank Nancy Gibson, Martin Ryan and Jean Flanagan for animal care, and Min-Ching Kuo and Alyssa Carey for technical assistance. This work was supported by Dartmouth College (Dartmouth Fellowship to JMG and JEC, and start-up funds to MvdM) and the Natural Sciences and Engineering Research Council (NSERC) of Canada (Discovery Grant award to MvdM, Canada Graduate Scholarship to JMG).

Conflict of Interest: The authors declare no competing financial interests.

1 Abstract

2 The nucleus accumbens (NAc) has been shown to be important for learning from feedback, and biasing and
3 invigorating behavior in response to outcome-predictive cues. NAc encodes outcome-related cue features
4 such as the magnitude and identity of reward. However, not much is known about how features of cues
5 themselves are encoded. We designed a decision making task where rats learned multiple sets of outcome-
6 predictive cues, and recorded single-unit activity in the NAc during performance. We found that coding
7 of various cue features occurred alongside coding of expected outcome. Furthermore, this coding persisted
8 during a delay period, after the rat made a decision and was waiting for an outcome, but not after the outcome
9 was revealed. Encoding of cue features in the NAc may enable contextual modulation of ongoing behavior,
10 and provide an eligibility trace of outcome-predictive stimuli for updating stimulus-outcome associations to
11 inform future behavior.

12 Introduction

13 Theories of nucleus accumbens (NAc) function generally agree that this brain structure contributes to moti-
14 vated behavior, with some emphasizing a role in learning from RPEs (Averbeck and Costa 2017; Joel, Niv,
15 and Ruppin 2002; Khamassi and Humphries 2012; Lee, Seo, and Jung 2012; Maia 2009; Schultz 2016; see
16 also the addiction literature on effects of drug rewards; Carelli 2010; Hyman, Malenka, and Nestler 2006;
17 Kalivas and Volkow 2005) and others a role in the modulation of ongoing behavior through stimuli associ-
18 ated with motivationally relevant outcomes (invigorating, directing; Floresco, 2015; Nicola, 2010; Salamone
19 & Correa, 2012). These proposals echo similar ideas on the functions of the neuromodulator dopamine
20 (Berridge, 2012; Maia, 2009; Salamone & Correa, 2012; Schultz, 2016), with which the NAc is tightly
21 linked functionally as well as anatomically (Cheer et al., 2007; du Hoffmann & Nicola, 2014; Ikemoto,
22 2007; Takahashi, Langdon, Niv, & Schoenbaum, 2016).

23 Much of our understanding of NAc function comes from studies of how cues that predict motivationally
24 relevant outcomes (e.g. reward) influence behavior and neural activity in the NAc. Task designs that associate
25 such cues with rewarding outcomes provide a convenient access point eliciting conditioned responses such as
26 sign-tracking and goal-tracking (Hearst & Jenkins, 1974; Robinson & Flagel, 2009), pavlovian-instrumental
27 transfer (Estes, 1943; Rescorla & Solomon, 1967) and enhanced response vigor (Nicola, 2010; Niv, Daw,
28 Joel, & Dayan, 2007), which tend to be affected by NAc manipulations (Chang, Wheeler, and Holland 2012;
29 Corbit and Balleine 2011; Flagel et al. 2011; although not always straightforwardly; Chang and Holland
30 2013; Giertler, Bohn, and Hauber 2004). Similarly, analysis of RPEs typically proceeds by establishing an
31 association between a cue and subsequent reward, with NAc responses transferring from outcome to the
32 cue with learning (Day, Roitman, Wightman, & Carelli, 2007; Roitman, Wheeler, & Carelli, 2005; Schultz,
33 Dayan, & Montague, 1997; Setlow, Schoenbaum, & Gallagher, 2003).

34 Surprisingly, although substantial work has been done on the coding of outcomes predicted by such cues
35 (Atallah, McCool, Howe, & Graybiel, 2014; Bissonette et al., 2013; Cooch et al., 2015; Day, Wheeler,

36 Roitman, & Carelli, 2006; Goldstein et al., 2012; Hollerman, Tremblay, & Schultz, 1998; Lansink et al.,
37 2012; McGinty, Lardeux, Taha, Kim, & Nicola, 2013; Nicola, 2004; Roesch, Singh, Brown, Mullins, &
38 Schoenbaum, 2009; Roitman et al., 2005; Saddoris, Stamatakis, & Carelli, 2011; Setlow et al., 2003; Sugam,
39 Saddoris, & Carelli, 2014; West & Carelli, 2016), much less is known about how outcome-predictive cues
40 themselves are encoded in the NAc (but see; Sleezer, Castagno, & Hayden, 2016). This is an important issue
41 for at least two reasons. First, in reinforcement learning, motivationally relevant outcomes are typically
42 temporally delayed relative to the cues that predict them. In order to solve the problem of assigning credit
43 (or blame) across such temporal gaps, some trace of preceding activity needs to be maintained (Lee et al.,
44 2012; Sutton & Barto, 1998). For example, if you become ill after eating food X in restaurant A, depending
45 on if you remember the identity of the restaurant or the food at the time of illness, you may learn to avoid
46 all restaurants, restaurant A only, food X only, or the specific pairing of X-in-A. Therefore, a complete
47 understanding of what is learned following feedback requires understanding what trace is maintained. Since
48 NAc is a primary target of DA signals interpretable as reward prediction errors (RPEs), and NAc lesions
49 impair RPEs related to timing, its activity trace will help determine what can be learned when RPEs arrive
50 (Hamid et al., 2015; Hart, Rutledge, Glimcher, & Phillips, 2014; Ikemoto, 2007; McDannald, Lucantonio,
51 Burke, Niv, & Schoenbaum, 2011; Takahashi et al., 2016).

52 Second, for ongoing behavior, the relevance of cues typically depends on context. In experimental set-
53 tings, context may include the identity of a preceding cue, spatial or configural arrangements (Bouton, 1993;
54 Holland, 1992; Honey, Iordanova, & Good, 2014), and unsignaled rules as occurs in set shifting and other
55 cognitive control tasks (Cohen & Servan-Schreiber, 1992; Floresco, Ghods-Sharifi, Vexelman, & Magyar,
56 2006; Grant & Berg, 1948; Sleezer et al., 2016). In such situations, the question arises how selective, context-
57 dependent processing of outcome-predictive cues is implemented. For instance, is there a gate prior to NAc
58 such that only currently relevant cues are encoded in NAc, or are all cues represented in NAc but their current
59 values dynamically updated (FitzGerald, Schwartenbeck, & Dolan, 2014; Goto & Grace, 2008; Sleezer et
60 al., 2016). Representation of cue identity would allow for context-dependent mapping of outcomes predicted
61 by specific cues.

62 Thus, both from a learning and a flexible performance perspective, it is of interest to determine how cue
63 identity is represented in the brain, with NAc of particular interest given its anatomical and functional po-
64 sition at the center of motivational systems. We sought to determine whether cue identity is represented in
65 the NAc, if cue identity is represented alongside other motivationally relevant variables, such as cue value,
66 and if these representations are maintained after a behavioral decision has been made (Figure 1). To address
67 these questions, we recorded the activity of NAc units as rats performed a task in which multiple, distinct
68 sets of cues predicted the same outcome.

69 [Figure 1 about here.]

70 **Methods**

71 **Subjects:**

72 Adult male Long-Evans rats ($n = 4$, Charles River, Saint Constant, QC) were used as subjects. Rats were in-
73 dividually housed with a 12/12-h light-dark cycle, and tested during the light cycle. Rats were food deprived
74 to 85-90% of their free feeding weight (weight at time of implantation was 440 - 470 g), and water restricted
75 4-6 hours before testing. All experimental procedures were approved by the the University of Waterloo An-
76 imal Care Committee (protocol# 11-06) and carried out in accordance with Canadian Council for Animal
77 Care (CCAC) guidelines.

78 **Overall timeline:**

79 Each rat was first handled for seven days during which they were exposed to the experiment room, the
80 sucrose solution used as a reinforcer, and the click of the sucrose dispenser valves. Rats were then trained

81 on the behavioral task (described in the next section) until they reached performance criterion. At this point
82 they underwent hyperdrive implantation targeted at the NAc. Rats were allowed to recover for a minimum
83 of five days before being retrained on the task, and recording began once performance returned to pre-
84 surgery levels. Upon completion of recording, animals were glosed, euthanized and recording sites were
85 histologically confirmed.

86 **Behavioral task and training:**

87 The behavioral apparatus was an elevated, square-shaped track (100 x 100 cm, track width 10 cm) containing
88 four possible reward locations at the end of track “arms” (Figure 2). Rats initiated a *trial* by triggering a
89 photobeam located 24 cm from the start of each arm. Upon trial initiation, one of two possible light cues
90 (L1, L2), or one of two possible sound cues (S1, S2), was presented that signaled the presence (*reward-*
91 *available trial*, L1+, S1+) or absence (*reward-unavailable trial*, L2-, S2-) of a 12% sucrose water reward
92 (0.1 mL) at the upcoming reward site. A trial was classified as an *approach trial* if the rat turned left at the
93 decision point and made a nosepoke at the reward receptacle (40 cm from the decision point), while trials
94 were classified as a *skip trial* if the rat instead turned right at the decision point and triggered the photobeam
95 to initiate the next trial. A trial is labeled *correct* if the rat approached (i.e. nosepoked) on reward-available
96 trials, and skipped (i.e. did not nosepoke) on reward-unavailable trials. On reward-available trials there
97 was a 1 second delay between a nosepoke and subsequent reward delivery. *Trial length* was determined by
98 measuring the length of time from cue onset until nosepoke (for approach trials), or from cue onset until
99 the start of the following trial (for skip trials). Trials could only be initiated through clockwise progression
100 through the series of arms, and each entry into the subsequent arm on the track counted as a trial.

101 Each session consisted of both a *light block* and a *sound block* with 100 trials each. Within a block, one cue
102 signaled reward was available on that trial (L1+ or S1+), while the other signaled reward was not available
103 (L2- or S2-). Light block cues were a flashing white light, and a constant yellow light. Sound block cues
104 were a 2 kHz sine wave and a 8 kHz sine wave whose amplitude was modulated from 0 to maximum by

105 a 2 Hz sine wave. Outcome-cue associations were counterbalanced across rats, e.g. for some rats L1+ was
106 the flashing white light, and for others L1+ was the constant yellow light. The order of cue presentation
107 was pseudorandomized so that the same cue could not be presented more than twice in a row. Block order
108 within each day was also pseudorandomized, such that the rat could not begin a session with the same block
109 for more than two days in a row. Each session consisted of a 5 minute pre-session period on a pedestal (a
110 terracotta planter filled with towels), followed by the first block, then the second block, then a 5 minute post-
111 session period on the pedestal. For approximately the first week of training, rats were restricted to running
112 in the clockwise direction by presenting a physical barrier to running counterclockwise. Cues signaling the
113 availability and unavailability of reward, as described above, were present from the start of training. Rats
114 were trained for 200 trials per day (100 trials per block) until they discriminated between the reward-available
115 and reward-unavailable cues for both light and sound blocks for three consecutive days, according to a chi-
116 square test rejecting the null hypothesis of equal approaches for reward-available and reward-unavailable
117 trials, at which point they underwent electrode implant surgery.

118 [Figure 2 about here.]

119 **Surgery:**

120 Surgical procedures were as described previously (Malhotra, Cross, Zhang, & van der Meer, 2015). Briefly,
121 animals were administered analgesics and antibiotics, anesthetized with isoflurane, induced with 5% in med-
122 ical grade oxygen and maintained at 2% throughout the surgery (0.8 L/min). Rats were then chronically
123 implanted with a “hyperdrive” consisting of 16 independently drivable tetrodes, either all 16 targeted for the
124 right NAc (AP +1.4 mm and ML +1.6 mm relative to bregma; Paxinos and Watson 1998), or 12 in the right
125 NAc and 4 targeted at the mPFC (AP +3.0 mm and ML +0.6 mm, relative to bregma; only data from NAc
126 tetrodes was analyzed). Following surgery, all animals were given at least five days to recover while receiv-
127 ing post-operative care, and tetrodes were lowered to the target (DV -6.0 mm) before being reintroduced to
128 the behavioral task.

129 **Data acquisition and preprocessing:**

130 After recovery, rats were placed back on the task for recording. NAc signals were acquired at 20 kHz with
131 a RHA2132 v0810 preamplifier (Intan) and a KJE-1001/KJD-1000 data acquisition system (Amplipex).
132 Signals were referenced against a tetrode placed in the corpus callosum above the NAc. Candidate spikes
133 for sorting into putative single units were obtained by band-pass filtering the data between 600-9000 Hz,
134 thresholding and aligning the peaks (UltraMegaSort2k, Hill, Mehta, & Kleinfeld, 2011). Spike waveforms
135 were then clustered with KlustaKwik using energy and the first derivative of energy as features, and manually
136 sorted into units (MClust 3.5, A.D. Redish et al., <http://redishlab.neuroscience.umn.edu/MClust/MClust.html>).
137 Isolated units containing a minimum of 200 spikes within a session were included for subsequent analysis.
138 Units were classified as fast spiking interneurons (FSIs) by an absence of interspike intervals (ISIs) > 2 s,
139 while medium spiny neurons (MSNs) had a combination of ISIs > 2 s and phasic activity with shorter ISIs
140 (Atallah et al., 2014; Barnes, Kubota, Hu, Jin, & Graybiel, 2005).

141 **Data analysis:**

142 *Behavior.* To determine if rats distinguished behaviorally between the reward-available and reward-unavailable
143 cues (*cue outcome*), we generated linear mixed effects models to investigate the relationships between cue
144 type and our behavioral variables, with *cue outcome* (reward available or not) and *cue identity* (light or
145 sound) as fixed effects, and the addition of an intercept for rat identity as a random effect. For each cue,
146 the average proportion of trials approached and trial length for a session were used as response variables.
147 Contribution of cue outcome to behavior was determined by comparing the full model to a model with cue
148 outcome removed for each behavioral variable.

149 *Neural data.* To investigate the contribution of different cue features (cue identity and cue outcome) on the
150 firing rates of NAc single units, we first determined whether firing rates for a unit were modulated by the
151 onset of a cue by collapsing across all cues and comparing the firing rates for the 1 s preceding cue-onset

152 with the 1 s following cue-onset. Single units were considered to be *cue-modulated* if a Wilcoxon signed-
153 rank test comparing pre- and post-cue firing was significant at $p < .01$. Cue-modulated units were then
154 classified as either increasing or decreasing if the post-cue activity was higher or lower than the pre-cue
155 activity, respectively.

156 To determine the relative contribution of different task parameters to firing rate variance (as in Figures 5-6),
157 a forward selection stepwise general linear model (GLM) was fit to each cue-modulated unit. Cue identity
158 (light block, sound block), cue location (arm 1, arm 2, arm 3, arm 4), cue outcome (reward-available, reward-
159 unavailable), behavior (approach, skip), trial length, trial number, and trial history (reward availability on the
160 previous 2 trials) were used as predictors, and the 1 s post-cue firing rate as the response variable. Units were
161 classified as being modulated by a given task parameter if addition of the parameter significantly improved
162 model fit using deviance as the criterion ($p < .01$). A comparison of the R-squared value between the final
163 model and the final model minus the predictor of interest was used to determine the amount of firing rate
164 variance explained by the addition of that predictor for a given unit. To investigate more finely the temporal
165 dynamics of the influence of task parameters to unit activity, we then fit a sliding window GLM with the
166 same task parameters using 500 ms bins and 100 ms steps, starting 500 ms before cue-onset, up to 500
167 ms after cue-onset, and measured the proportion of units and average R-squared value for a given time bin
168 where a particular predictor contributed significantly to the final model. To control for the amount of units
169 that would be affected by a predictor by chance, we shuffled the trial order of firing rates for a particular unit
170 within a time bin, and took the average of this value over 100 shuffles.

171 To better visualize responses to cues and enable subsequent population level analyses (as in Figures 5, 7,
172 and 8), spike trains were convolved with a Gaussian kernel ($\sigma = 100$ ms), and peri-event time histograms
173 (PETHs) were generated by taking the average of the convolved spike trains across all trials for a given
174 task condition. For analysis of population-level responses for cue features (Figure 7), convolved spike trains
175 for all units where cue identity, cue location, or cue outcome explained a significant portion of firing rate
176 variance were z-scored. Within a given cue feature, normalized spike trains were then separated according

177 to the preferred and non-preferred cue condition (e.g. light vs. sound block), and averaged across units to
178 generate population-level averages. To account for separation that would result from any random selection
179 of units, unit identity was shuffled and the shuffled average for preferred and non-preferred cue conditions
180 was generated for 1000 shuffles.

181 To visualize NAc representations of task space within cue conditions, normalized spike trains for all units
182 were ordered by the location of their maximum or minimum firing rate for a specified cue condition (Figure
183 8). To compare representations of task space across cue conditions for a cue feature, the ordering of units
184 derived for one condition (e.g. light block) was then applied to the normalized spike trains for the other
185 condition (e.g. sound block). For control comparisons within cue conditions, half of the trials for a condition
186 were compared against the other half. To look at the correlation of firing rates of all units within and across
187 various cue conditions, trials for each cue condition for a unit were shuffled and divided into two averages,
188 and averages within and across cue conditions were correlated. A linear mixed effects model was run for
189 each cue condition to determine if correlations of firing rates within cue conditions were more similar than
190 correlations across cue conditions.

191 To identify the responsivity of units to different cue features at the time of a nosepoke into a reward re-
192 ceptacle, and subsequent reward delivery, the same cue-responsive units from the cue-onset analyses were
193 analyzed at the time of nosepoke and outcome receipt using identical analysis techniques (Figures 9, 10, 11,
194 and 12).

195 Given that some of our analyses compare firing rates across time, particularly comparisons across blocks,
196 we sought to exclude units with unstable firing rates that would generate spurious results reflecting a drift
197 in firing rate over time unrelated to our task. To do this we ran a Mann-Whitney U test comparing the
198 cue-evoked firing rates for the first and second half of trials within a block, and excluded 99 of 443 units
199 from analysis that showed a significant change for either block, leaving 344 units for further analyses.
200 All analyses were completed in MATLAB R2015a, the code is available on our public GitHub repository

201 (<http://github.com/vandermeerlab/papers>), and the data can be accessed through DataLad.

202 **Histology:**

203 Upon completion of the experiment, recording channels were glosed by passing $10 \mu A$ current for 10 sec-
204 onds and waiting 5 days before euthanasia, except for rat R057 whose implant detached prematurely. Rats
205 were anesthetized with 5% isoflurane, then asphyxiated with carbon dioxide. Transcardial perfusions were
206 performed, and brains were fixed and removed. Brains were sliced in $50 \mu m$ coronal sections and stained
207 with thionin. Slices were visualized under light microscopy, tetrode placement was determined, and elec-
208 trodes with recording locations in the NAc were analyzed (Figure 3).

209 [Figure 3 about here.]

210 **Results**

211 **Behavior**

212 Rats were trained to discriminate between cues signaling the availability and absence of reward on a square
213 track with four identical arms for two distinct set of cues (Figure 2). During each session, rats were pre-
214 sented sequentially with two behavioral blocks containing cues from different sensory modalities, a light and
215 a sound block, with each block containing a cue that signalled the availability of reward (reward-available),
216 and a cue that signalled the absence of reward (reward-unavailable). To maximize reward receipt, rats should
217 approach reward sites on reward-available trials, and skip reward sites on reward-unavailable trials (see Fig-
218 ure 4A for an example learning curve). All four rats learned to discriminate between the reward-available
219 and reward-unavailable cues for both the light and sound blocks as determined by reaching significance ($p <$

.05) on a daily chi-square test comparing approach behavior for reward-available and reward-unavailable cues for each block, for at least three consecutive days (range for time to criterion: 22 - 57 days). Maintenance of behavioral performance during recording sessions was assessed using linear mixed effects models for both proportion of trials where the rat approached the receptacle, and trial length. Analyses revealed that the likelihood of a rat to make an approach was influenced by whether a reward-available or reward-unavailable cue was presented, but was not significantly modulated by whether the rat was presented with a light or sound cue (Percentage approached: light reward-available = 97%; light reward-unavailable = 34%; sound reward-available = 91%; sound reward-unavailable 35%; cue identity p = .115; cue outcome p < .001; Figure 4B). A similar trend was seen with the length of time taken to complete a trial (Trial length: light reward-available = 1.85 s; light reward-unavailable = 1.74 s; sound reward-available = 1.91 s; sound reward-unavailable 1.78 s; cue identity p = .106; cue outcome p < .001; Figure 4C). Thus, during recording, rats successfully discriminated the cues according to whether or not they signaled the availability of reward at the reward receptacle.

[Figure 4 about here.]

234 NAc units encode behaviorally relevant and irrelevant cue features

235 Single unit responses discriminate cue features:

236 We sought to address which parameters of our task were encoded by NAc activity, specifically whether
237 the NAc encodes aspects of motivationally relevant cues not directly tied to reward, such as the identity
238 and location of the cue, and whether this coding is independent or integrated with coding of cue outcome.
239 To do this we recorded a total of 443 units with > 200 spikes in the NAc from 4 rats over 57 sessions
240 while they performed a cue discrimination task (Table 1). Units that exhibited a drift in firing rate over
241 the course of either block were excluded from further analysis, leaving 344 units for further analysis. The

activity of 133 (39%) of these 344 units were modulated by the cue, with more showing a decrease in firing (n = 103) than an increase (n = 30) around the time of cue-onset (Table 1). Within this group, 24 were classified as FSIs, while 109 were classified as SPNs. Upon visual inspection, we observed several patterns of firing activity, including units that discriminated firing upon cue-onset across various cue conditions, showed sustained differences in firing across cue conditions, had transient responses to the cue, showed a ramping of activity starting at cue-onset, and showed elevated activity immediately preceding cue-onset, for example (Figure 5). To characterize more formally whether these cue-evoked responses were modulated by various aspects of the task, we fit a GLM to each cue-modulated unit. Fitting GLMs revealed that a variety of task parameters accounted for a significant portion of firing rate variance in NAc cue-modulated units (Figure 6, Table 1). Notably, there were units that discriminated between whether the rat was performing in the light or sound block (28% of cue-modulated units, accounting for 6% of variance on average), which arm the rat was currently on (38% of cue-modulated units, accounting for 6% of variance on average), and whether the rat was engaged in the common portion of a reward-available or reward-unavailable trial (26% of cue-modulated units, accounting for 4% of variance on average), suggesting that the NAc encodes features of reward-predictive cues separate from expected outcome (Figure 5A-F). Furthermore, overlap of coding of cue features within units was not different than expected by chance according to chi-square tests, suggesting for integrated coding across various aspects of a cue (Figure 5G,H). Additionally, a sliding window GLM centered on cue-onset revealed that cue identity and cue location contributed to the activity of a significant proportion of cue-modulated units throughout this epoch, whereas an increase in units encoding cue outcome became apparent after cue-onset (Figure 6D). Together, these findings show that various cue features are represented in the NAc, and that this coding is both integrated and separate from expected outcome (Figure 1; H2,H3).

[Table 1 about here.]

[Figure 5 about here.]

266

[Figure 6 about here.]

267 **Population level averages reveal characteristic response profiles:**

268 We observed a variety of single unit response profiles around the time of cue onset (Figure 5). To investigate
269 whether these firing rate patterns were related to what cue features were encoded, we plotted the population
270 level averages for units that were modulated by each feature. To do this, we normalized firing activity for
271 each unit that was modulated by a given cue feature, such as light block, then generated the cue-onset aligned
272 population average firing rate for each of the cue features (Figure 7). Overall, this analysis revealed that cells
273 that showed an increase upon cue presentation had stronger responses for the preferred cue condition (Figure
274 7A,C,E). Interestingly, units that were classified as decreasing in response to the cue showed a biphasic
275 response at the population level, with a small peak at a time in alignment with entry into the arm, followed by
276 a sustained dip after cue-onset (Figure 7B,D,F). Units that were modulated by cue identity showed a stronger
277 increase in response to the preferred task block, as well as a higher tonic firing rate to the preferred task block,
278 most notably in units that decreased in firing rate to the cue (Figure 7A,B). Units that were modulated by cue
279 location showed a graded response to locations of decreasing preference, with peak firing occurring around
280 cue-onset (Figure 7C,D). Units that were modulated by cue outcome showed a ramping of activity after
281 cue-onset for their preferred cue type. Additionally, units that exhibited a decrease in firing in response to
282 the cue and whose activity was modulated by cue outcome, showed a sustained discriminatory response to
283 reward-available and reward-unavailable cues that extended beyond cue-onset (Figure 7F). Together, these
284 visualizations of the averaged population responses revealed nuanced differences in the way NAc units are
285 modulated by cue conditions across cue features.

286

[Figure 7 about here.]

287 **NAc units dynamically segment the task:**

Given the varied time courses and response profiles of NAc units to various aspects of the cue, the NAc may be computing a temporally evolving state value signal (Pennartz., 2011). If this is the case, then the recruitment of NAc units should vary alongside changes in the environment. To look at the distribution of responses throughout our task space and see if this distribution is modulated by cue features, we z-scored the firing rate of each unit and plotted the normalized firing rates of all units aligned to cue-onset and sorted them according to the time of peak firing rate (Figure 8). We did this separately for both the light and sound blocks, and found a nearly uniform distribution of firing fields in task space that was not limited to alignment to the cue (Figure 8A). Furthermore, to determine if this population level activity was similar across blocks, we also organized firing during the sound blocks according to the ordering derived from the light blocks. This revealed that while there was some preservation of order, the overall firing was qualitatively different across the two blocks, implying that population activity distinguishes between light and sound blocks. To control for the possibility that any comparison of trials would produce this effect, we did a within block comparison, comparing half of the trials in the light block against the other half. This comparison looked similar to our test comparison of sound block trials ordered by light block trials. Additionally, given that the majority of our units showed an inhibitory response to the cue, we also plotted the firing rates according to the lowest time in firing, and again found some maintenance of order, but largely different ordering across the two blocks, and the within block comparison (Figure 8D). To further test this, we divided each block into two halves and looked at the correlation of the average smoothed firing rates across various combinations of these halves across our cue-aligned centered epoch. A linear mixed effects model revealed that within block correlations (e.g. one half of light trials vs other half of light trials) were higher and more similar than across block correlations (e.g. half of light trials vs half of sound trials) suggesting that activity in the NAc discriminates across various cue conditions (within block correlations = .383 (light), .379 (sound); across block correlations = .343, .338, .337, .348; within block vs. within block comparison = $p = .934$; within block vs. across block comparisons = $p < .001$). This process was repeated for cue location (Figure 8B,E; within block correlations = .369 (arm 1), .350 (arm 2); across block correlations = .290, .286, .285, .291; within block vs. within block comparison = $p = .071$; within block vs. across block comparisons = $p < .001$) and cue outcome (Figure 8C,F; within block correlations = .429 (reward-available), .261 (reward-unavailable); across block correlations = .258, .253, .255, .249; within block vs. within block comparison

316 = $p < .001$; within block vs. across block comparisons = $p < .001$), showing that NAc segmentation of the
317 task is qualitatively different even during those parts of the task not immediately associated with a specific
318 cue, action, or outcome, although the within condition comparison of reward-unavailable trials was less
319 correlated than reward-available trials, and more similar to the across condition comparisons, potentially due
320 to the greater behavioral variability for the reward-unavailable trials.

321 [Figure 8 about here.]

322 **Encoding of cue features persists until outcome:**

323 In order to be useful for credit assignment in reinforcement learning, a trace of the cue must be maintained
324 until the outcome, so that information about the outcome can be associated with the outcome-predictive
325 cue. To test whether representations of cue features persisted post-approach until the outcome was revealed,
326 we fit a GLM to the post-approach firing rates of cue-modulated units aligned to the time of nosepoke into
327 the reward receptacle. This analysis showed that a variety of units still discriminated firing according to
328 various cue features, but not other task parameters, showing that NAc activity discriminates various cue
329 conditions well into a trial (Table 1, Figures 9,10). Additionally, these units were a mix between most of the
330 units that encoded cue features at cue-onset (observed overlap greater than expected by chance according
331 to chi-square tests), and those that did not previously have a cue feature as a predictor (29, 48, and 30
332 out of 133 cue-modulated units encoded both time points for cue identity, cue location, and cue outcome,
333 respectively). Population level averages for units that increased to cue-onset showed a ramping up of activity
334 that peaked upon nosepoke, whereas units that decreased to cue-onset showed a gradual reduction of firing
335 activity that reached a minimum upon nosepoke (Figure 11). Additionally, a peak is seen for preferred
336 cue outcome in decreasing units at 1 second post cue-onset when reward was received, demonstrating an
337 integration of expected and received reward (Figure 11F). Furthermore, aligning normalized peak firing rates
338 to nosepoke onset, revealed a clustering of responses around outcome receipt for all cue conditions where the
339 rat would have received reward (Figure 12), in addition to the same trend of higher within- vs across-block

correlations for cue identity (Figure 12A,C; within block correlations = .560 (light), .541 (sound); across block correlations = .487, .481, .483, .486; within block vs. within block comparison = $p = .112$; within block vs. across block comparisons = $p < .001$) and cue location (Figure 12B,E; within block correlations = .474 (arm 1), .461 (arm 2); across block correlations = .416, .402, .416, .415; within block vs. within block comparison = $p = .810$; within block vs. across block comparisons = $p < .001$), but not cue outcome (Figure 12C,F; within block correlations = .620 (reward-available), .401 (reward-unavailable); across block correlations = .418, .414, .390, .408; within block vs. within block comparison = $p < .001$; within block vs. across block comparisons = $p < .001$). To determine whether coding of cue features persisted after the outcome was revealed, a GLM was fit to the firing rates of cue-modulated units at the time of outcome receipt, during which the cue was still present. Fitting a GLM revealed 10 units (8%) where cue outcome accounted for an average of 32% of firing rate variance (Table 1, data not shown). An absence of cue identity or cue location coding at this level of analysis was observed, but looking at the data more closely with a sliding window GLM revealed that cue identity, cue location, and cue outcome were encoded throughout time epochs surround cue-onset, nosepoke hold, and outcome receipt, suggesting that the NAc maintains a representation of these cue features once the rat receives behavioral feedback for its decision (Figure 10E-J).

[Figure 9 about here.]

[Figure 10 about here.]

[Figure 11 about here.]

[Figure 12 about here.]

359 **Discussion**

360 The main result of the present study is that NAc units encode not only the expected outcome of outcome-
361 predictive cues, but also the identity of such cues. Importantly, this identity coding was maintained on
362 approach trials during a delay period where the rat held a nosepoke until the outcome was received (H2 in
363 Figure 1B). Units coding for cue identity showed partial overlap with those coding for expected outcome
364 (H3 in Figure 1A). Units that coded different cue features (identity, outcome, location) exhibited different
365 temporal profiles as a whole, although across all recorded units a tiling of task structure was observed such
366 that all points within our analyzed task space was accounted for by the ordered peak firing rates of all units.
367 Furthermore, this tiling differed between various conditions with a cue feature, such as light versus sound
368 blocks. We discuss these observations and their implications below.

369 **Cue identity:**

370 Our finding that NAc units can discriminate between different outcome-predictive stimuli with similar moti-
371 vational significance (i.e. encodes cue identity) expands upon an extensive rodent literature examining NAc
372 correlates of conditioned stimuli (Ambroggi, Ishikawa, Fields, & Nicola, 2008; Atallah et al., 2014; Bis-
373 sonette et al., 2013; Cooch et al., 2015; Day et al., 2006; Dejean et al., 2017; Goldstein et al., 2012; Ishikawa,
374 Ambroggi, Nicola, & Fields, 2008; Lansink et al., 2012; McGinty et al., 2013; Nicola, 2004; Roesch et al.,
375 2009; Roitman et al., 2005; Saddoris et al., 2011; Setlow et al., 2003; Sugam et al., 2014; West & Carelli,
376 2016; Yun, Wakabayashi, Fields, & Nicola, 2004). Perhaps the most comparable work in rodents comes
377 from a study that found distinct coding for an odor when it predicted separate but equally valued rewards
378 (Cooch et al., 2015). The present work is complementary to such *outcome identity* coding as it shows that
379 NAc units *cue identity*, both separately and integrated with the reward it predicts (H2 and H3 in Figure 1A).
380 Similarly, Setlow et al. 2003 paired distinct cues with appetitive or aversive outcomes, and found separate
381 populations of units that encoded each cue. Once again, our study was different in asking how distinct cues
382 encoding the same anticipated outcome are encoded. Such cue identity encoding suggests that even when

383 the biological relevance of these stimuli is similar, NAc dissociates their representations at the level of the
384 single-units. A possible interpretation of this coding of cue features alongside expected outcome is that these
385 representations are used to associate reward with relevant features of the environment, so-called credit as-
386 signment in the reinforcement learning literature (Sutton & Barto, 1998). A burgeoning body of human and
387 non-human primate work has started to elucidated neural correlates of credit assignment in the PFC, partic-
388 ularly in the lateral orbitofrontal cortex (Akaishi, Kolling, Brown, & Rushworth, 2016; Asaad, Lauro, Perge,
389 & Eskandar, 2017; Chau et al., 2015; Noonan, Chau, Rushworth, & Fellows, 2017). Given the importance of
390 cortical inputs in NAc associative representations, it is possible that information related to credit assignment
391 is relayed from the cortex to NAc (Cooch et al., 2015; Ishikawa et al., 2008).

392 A different possible function for cue identity coding is to support contextual modulation of the motivational
393 relevance of specific cues. A context can be understood as a particular mapping between specific cues and
394 their outcomes: for instance, in context 1 cue A but not cue B is rewarded, whereas in context 2 cue B but
395 not cue A is rewarded. Successfully implementing such contextual mappings requires representation of the
396 cue identities. Indeed, Sleezer et al. 2016 recorded NAc responses during the Wisconsin Card Sorting Task
397 (WCST), a common set-shifting task used in both the laboratory and clinic, and found units that preferred
398 firing to stimuli when a certain rule, or rule category was currently active. Further support for a modulation
399 of NAc responses by strategy comes from an fMRI study that examined BOLD levels during a set-shifting
400 task (FitzGerald et al., 2014). In this task, participants learned two sets of stimulus-outcome contingencies,
401 a visual set and auditory set. During testing they were presented with both simultaneously, and the stimulus
402 dimension that was relevant was periodically shifted between the two. Here, they found that bilateral NAc
403 activity reflected value representations for the currently relevant stimulus dimension, and not the irrelevant
404 stimulus. The current finding of separate, but overlapping, populations of units encoding cue identity and
405 expected outcome, suggests that the fMRI finding is generated by the combined activity of several different
406 functional cell types.

407 Our analyses were designed to eliminate several potential alternative interpretations to cue identity coding.

408 Because the different cues were separated into different blocks, units that discriminated between cue identi-
409 ties could instead be encoding time or other slowly-changing quantities. We excluded this possible confound
410 by excluding units that showed a drift in firing between the first and second half within a block. However, the
411 possibility remains that instead of or in addition to stimulus identity, these units encode a preferred context,
412 or even a macroscale representation of progress through the session. Indeed, encoding of the current strategy
413 could be an explanation for the sustained difference in population averaged firing across stimulus blocks
414 (Figure 7), as well as a potential explanation for the differentially tiling of task structure across blocks in the
415 current study (Figure 8).

416 A different potential confound is that between outcome and action value coding. We discriminated between
417 these possibilities by analyzing error trials, where the rat approached reward (left turn) after presentation of
418 the reward-unavailable cue. Units that were modulated by the expected outcome of the cue maintained their
419 specific firing patterns even during error trials, as expected from outcome value coding but not action value
420 coding. Additionally, NAc signals have been shown to be modulated by response vigor (McGinty et al.,
421 2013); to detangle this from our results we included trial length (i.e. latency to arrival at the reward site) as a
422 predictor in our GLMs, and found units with cue feature correlates independent of trial length.

423 An overall limitation of the current study is that rats were never presented with both sets of cues simultane-
424 ously, and were not required to switch strategies between multiple sets of cues. Thus, it is unknown to what
425 extent the cue identity encoding we observed is behaviorally relevant, although extrapolating data from other
426 work (Sleeker et al., 2016) suggests that cue identity coding would be modulated by relevance. NAc core
427 lesions have been shown to impair shifting between different behavioral strategies (Floresco et al., 2006),
428 and it is possible that selectively silencing the units that prefer responding for a given modality or rule would
429 impair performance when the animal is required to use that information, or artificial enhancement of those
430 units would cause them to use the rule when it is the inappropriate strategy.

431 **Encoding of position:**

432 Our finding that cue-evoked activity was modulated by cue location is in alignment with several previous
433 reports (Lavoie & Mizumori, 1994; Mulder, Shibata, Trullier, & Wiener, 2005; Strait et al., 2016; Wiener
434 et al., 2003). The NAc receives inputs from the hippocampus, and the communication of place-reward in-
435 formation across the two structures suggests that the NAc tracks locations associated with reward (Lansink
436 et al., 2008; Lansink, Goltstein, Lankelma, McNaughton, & Pennartz, 2009; Lansink et al., 2016; Pennartz,
437 2004; Sjulson, Peyrache, Cumpelik, Cassataro, & Buzsáki, 2017; Tabuchi, Mulder, & Wiener, 2000; van der
438 Meer & Redish, 2011). NAc units can also signal progress through a sequence of cues and/or actions (Atal-
439 lah et al., 2014; Berke, Breck, & Eichenbaum, 2009; Khamassi, Mulder, Tabuchi, Douchamps, & Wiener,
440 2008; Lansink et al., 2012; Mulder, Tabuchi, & Wiener, 2004; Shidara, Aigner, & Richmond, 1998). Given
441 that the current task was pseudo-random, it is possible that the rats learned the structure of sequential cue
442 presentation, and the neural activity could reflect this. However, this is unlikely as including a previous trial
443 variable in the analysis did not explain a significant amount of firing rate variance in response to the cue for
444 the vast majority of units. In any case, NAc units on the present task continued to distinguish between differ-
445 ent locations, even though location, and progress through a sequence, were explicitly irrelevant in predicting
446 reward. We speculate that this persistent coding of location in NAc may represent a bias in credit assignment,
447 and associated tendency for rodents to associate motivationally relevant events with the locations where they
448 occur.

449 **Implications:**

450 Maladaptive decision making, as occurs in schizophrenia, addiction, Parkinson's, among others, can re-
451 sult from dysfunctional RPE and value signals (Frank, Seeberger, & O'Reilly, 2004; Gradin et al., 2011;
452 Maia & Frank, 2011). This view has been successful in explaining both positive and negative symptoms in
453 schizophrenia, and deficits in learning from feedback in Parkinson's (Frank et al., 2004; Gradin et al., 2011).
454 However, the effects of RPE and value updating are contingent upon encoding of preceding action and cue
455 features, the eligibility trace (Lee et al., 2012; Sutton & Barto, 1998). Value updates can only be performed
456 on these aspects of preceding experience that are encoded when the update occurs. Therefore, maladaptive

457 learning and decision making can result from not only aberrant RPEs but also from altered cue feature en-
458 coding. For instance, on this task the environmental stimulus that signaled the availability of reward was
459 conveyed by two distinct cues that were presented in four locations. While in our current study, the location
460 and identity of the cue did not require any adjustments in the animals behavior, we found coding of these
461 features alongside the expected outcome of the cue that could be the outcome of credit assignment compu-
462 tations computed upstream. Identifying neural coding related to an aspect of credit assignment is important
463 as inappropriate credit assignment could be a contributor to conditioned fear overgeneralization seen in dis-
464 orders with pathological anxiety such as generalized anxiety disorder, post traumatic stress disorder, and
465 obsessive-compulsive disorder (Kaczkurkin et al., 2017; Kaczkurkin & Lissek, 2013; Lissek et al., 2014),
466 and delusions observed in disorders such as schizophrenia, Alzheimer's and Parkinson's (Corlett, Taylor,
467 Wang, Fletcher, & Krystal, 2010; Kapur, 2003). Thus, our results provide a neural window into the process
468 of credit assignment, such that the extent and specific manner in which this process fails in syndromes such
469 as schizophrenia, obsessive-compulsive disorder, etc. can be experimentally accessed.

470 References

- 471 Akaishi, R., Kolling, N., Brown, J. W., & Rushworth, M. (2016). Neural Mechanisms of Credit Assignment in a Multicue
472 Environment. *Journal of Neuroscience*, 36(4), 1096–1112. doi: 10.1523/JNEUROSCI.3159-15.2016
- 473 Ambroggi, F., Ishikawa, A., Fields, H. L., & Nicola, S. M. (2008). Basolateral Amygdala Neurons Facilitate Reward-Seeking
474 Behavior by Exciting Nucleus Accumbens Neurons. *Neuron*, 59(4), 648–661. doi: 10.1016/j.neuron.2008.07.004
- 475 Asaad, W. F., Lauro, P. M., Perge, J. A., & Eskandar, E. N. (2017). Prefrontal Neurons Encode a Solution to the Credit-Assignment
476 Problem. *The Journal of Neuroscience*, 37(29), 6995–7007. doi: 10.1523/JNEUROSCI.3311-16.2017
- 477 Atallah, H. E., McCool, A. D., Howe, M. W., & Graybiel, A. M. (2014). Neurons in the ventral striatum exhibit cell-type-specific
478 representations of outcome during learning. *Neuron*, 82(5), 1145–1156. doi: 10.1016/j.neuron.2014.04.021
- 479 Averbeck, B. B., & Costa, V. D. (2017). Motivational neural circuits underlying reinforcement learning. *Nature Neuroscience*,
480 20(4), 505–512. doi: 10.1038/nn.4506
- 481 Barnes, T. D., Kubota, Y., Hu, D., Jin, D. Z., & Graybiel, A. M. (2005). Activity of striatal neurons reflects dynamic encoding and
482 recoding of procedural memories. *Nature*, 437(7062), 1158–1161. doi: 10.1038/nature04053

- 483 Berke, J. D., Breck, J. T., & Eichenbaum, H. (2009). Striatal Versus Hippocampal Representations During Win-Stay Maze Performance. *Journal of Neurophysiology*, 101(3), 1575–1587. doi: 10.1152/jn.91106.2008
- 484
- 485 Berridge, K. C. (2012). From prediction error to incentive salience: Mesolimbic computation of reward motivation. *European*
486 *Journal of Neuroscience*, 35(7), 1124–1143. doi: 10.1111/j.1460-9568.2012.07990.x
- 487 Bissonette, G. B., Burton, A. C., Gentry, R. N., Goldstein, B. L., Hearn, T. N., Barnett, B. R., ... Roesch, M. R. (2013). Separate
488 Populations of Neurons in Ventral Striatum Encode Value and Motivation. *PLoS ONE*, 8(5), e64673. doi: 10.1371/jour-
489 nal.pone.0064673
- 490 Bouton, M. E. (1993). Context, time, and memory retrieval in the interference paradigms of Pavlovian learning. *Psychological*
491 *Bulletin*, 114(1), 80–99. doi: 10.1371/journal.pone.0064673
- 492 Carelli, R. M. (2010). Drug Addiction: Behavioral Neurophysiology. In *Encyclopedia of neuroscience* (pp. 677–682). Elsevier.
493 doi: 10.1016/B978-008045046-9.01546-1
- 494 Chang, S. E., & Holland, P. C. (2013). Effects of nucleus accumbens core and shell lesions on autoshaped lever-pressing. *Be-*
495 *havioural Brain Research*, 256, 36–42. doi: 10.1016/j.bbr.2013.07.046
- 496 Chang, S. E., Wheeler, D. S., & Holland, P. C. (2012). Roles of nucleus accumbens and basolateral amygdala in autoshaped lever
497 pressing. *Neurobiology of Learning and Memory*, 97(4), 441–451. doi: 10.1016/j.nlm.2012.03.008
- 498 Chau, B. K. H., Sallet, J., Papageorgiou, G. K., Noonan, M. A. P., Bell, A. H., Walton, M. E., & Rushworth, M. F. S. (2015).
499 Contrasting Roles for Orbitofrontal Cortex and Amygdala in Credit Assignment and Learning in Macaques. *Neuron*, 87(5),
500 1106–1118. doi: 10.1016/j.neuron.2015.08.018
- 501 Cheer, J. F., Aragona, B. J., Heien, M. L. A. V., Seipel, A. T., Carelli, R. M., & Wightman, R. M. (2007). Coordinated
502 Accumbal Dopamine Release and Neural Activity Drive Goal-Directed Behavior. *Neuron*, 54(2), 237–244. doi:
503 10.1016/j.neuron.2007.03.021
- 504 Cohen, J. D., & Servan-Schreiber, D. (1992). Context, cortex, and dopamine: a connectionist approach to behavior and biology in
505 schizophrenia. *Psychological Review*, 99(1), 45. doi: 10.1016/j.neuron.2007.03.021
- 506 Cooch, N. K., Stalnaker, T. A., Wied, H. M., Bali-Chaudhary, S., McDannald, M. A., Liu, T. L., & Schoenbaum, G. (2015).
507 Orbitofrontal lesions eliminate signalling of biological significance in cue-responsive ventral striatal neurons. *Nature Com-*
508 *munications*, 6, 7195. doi: 10.1038/ncomms8195
- 509 Corbit, L. H., & Balleine, B. W. (2011). The General and Outcome-Specific Forms of Pavlovian-Instrumental Transfer Are
510 Differentially Mediated by the Nucleus Accumbens Core and Shell. *Journal of Neuroscience*, 31(33), 11786–11794. doi:
511 10.1523/JNEUROSCI.2711-11.2011
- 512 Corlett, P. R., Taylor, J. R., Wang, X.-J., Fletcher, P. C., & Krystal, J. H. (2010). Toward a neurobiology of delusions. *Progress in*
513 *Neurobiology*, 92, 345–369. doi: 10.1016/j.pneurobio.2010.06.007
- 514 Day, J. J., Roitman, M. F., Wightman, R. M., & Carelli, R. M. (2007). Associative learning mediates dynamic shifts in dopamine
515 signaling in the nucleus accumbens. *Nature Neuroscience*, 10(8), 1020–1028. doi: 10.1038/nn1923

- 516 Day, J. J., Wheeler, R. A., Roitman, M. F., & Carelli, R. M. (2006). Nucleus accumbens neurons encode Pavlovian approach behav-
517 iors: Evidence from an autoshaping paradigm. *European Journal of Neuroscience*, 23(5), 1341–1351. doi: 10.1111/j.1460-
518 9568.2006.04654.x
- 519 Dejean, C., Sitko, M., Girardeau, P., Bennabi, A., Caillé, S., Cador, M., ... Le Moine, C. (2017). Memories of Opiate Withdrawal
520 Emotional States Correlate with Specific Gamma Oscillations in the Nucleus Accumbens. *Neuropsychopharmacology*,
521 42(5), 1157–1168. doi: 10.1038/npp.2016.272
- 522 du Hoffmann, J., & Nicola, S. M. (2014). Dopamine Invigorates Reward Seeking by Promoting Cue-Evoked Excitation in the
523 Nucleus Accumbens. *Journal of Neuroscience*, 34(43), 14349–14364. doi: 10.1523/JNEUROSCI.3492-14.2014
- 524 Estes, W. K. (1943). Discriminative conditioning. I. A discriminative property of conditioned anticipation. *Journal of Experimental
525 Psychology*, 32(2), 150–155. doi: 10.1037/h0058316
- 526 Fitzgerald, T. H. B., Schwartenbeck, P., & Dolan, R. J. (2014). Reward-Related Activity in Ventral Striatum Is Action Contingent
527 and Modulated by Behavioral Relevance. *Journal of Neuroscience*, 34(4), 1271–1279. doi: 10.1523/JNEUROSCI.4389-
528 13.2014
- 529 Flagel, S. B., Clark, J. J., Robinson, T. E., Mayo, L., Czuj, A., Willuhn, I., ... Akil, H. (2011). A selective role for dopamine in
530 stimulus-reward learning. *Nature*, 469(7328), 53–59. doi: 10.1038/nature09588
- 531 Floresco, S. B. (2015). The Nucleus Accumbens: An Interface Between Cognition, Emotion, and Action. *Annual Review of
532 Psychology*, 66(1), 25–52. doi: 10.1146/annurev-psych-010213-115159
- 533 Floresco, S. B., Ghods-Sharifi, S., Vexelman, C., & Magyar, O. (2006). Dissociable roles for the nucleus accumbens core and shell
534 in regulating set shifting. *Journal of Neuroscience*, 26(9), 2449–2457. doi: 10.1523/JNEUROSCI.4431-05.2006
- 535 Frank, M. J., Seeberger, L. C., & O'Reilly, R. C. (2004). By carrot or by stick: Cognitive reinforcement learning in Parkinsonism.
536 *Science*, 306(5703), 1940–1943. doi: 10.1126/science.1102941
- 537 Giertler, C., Bohn, I., & Hauber, W. (2004). Transient inactivation of the rat nucleus accumbens does not impair guidance of
538 instrumental behaviour by stimuli predicting reward magnitude. *Behavioural Pharmacology*, 15(1), 55–63. doi: 10.1126/sci-
539 ence.1102941
- 540 Goldstein, B. L., Barnett, B. R., Vasquez, G., Tobia, S. C., Kashtelyan, V., Burton, A. C., ... Roesch, M. R. (2012). Ventral Striatum
541 Encodes Past and Predicted Value Independent of Motor Contingencies. *Journal of Neuroscience*, 32(6), 2027–2036. doi:
542 10.1523/JNEUROSCI.5349-11.2012
- 543 Goto, Y., & Grace, A. A. (2008). Limbic and cortical information processing in the nucleus accumbens. *Trends in Neurosciences*,
544 31(11), 552–558. doi: 10.1016/j.tins.2008.08.002
- 545 Gradin, V. B., Kumar, P., Waiter, G., Ahearn, T., Stickle, C., Milders, M., ... Steele, J. D. (2011). Expected value and prediction
546 error abnormalities in depression and schizophrenia. *Brain*, 134(6), 1751–1764. doi: 10.1093/brain/awr059
- 547 Grant, D. A., & Berg, E. (1948). A behavioral analysis of degree of reinforcement and ease of shifting to new responses in a
548 Weigl-type card-sorting problem. *Journal of Experimental Psychology*, 38(4), 404–411. doi: 10.1037/h0059831

- 549 Hamid, A. A., Pettibone, J. R., Mabrouk, O. S., Hetrick, V. L., Schmidt, R., Vander Weele, C. M., ... Berke, J. D. (2015).
550 Mesolimbic dopamine signals the value of work. *Nature Neuroscience*, 19(1), 117–126. doi: 10.1038/nn.4173
- 551 Hart, A. S., Rutledge, R. B., Glimcher, P. W., & Phillips, P. E. M. (2014). Phasic Dopamine Release in the Rat Nucleus Accumbens Symmetrically Encodes a Reward Prediction Error Term. *The Journal of Neuroscience*, 34(3), 698–704. doi:
552 10.1523/JNEUROSCI.2489-13.2014
- 553
- 554 Hearst, E., & Jenkins, H. M. (1974). *Sign-tracking: the stimulus-reinforcer relation and directed action*. Psychonomic Society.doi:
555 10.1523/JNEUROSCI.2489-13.2014
- 556 Hill, D. N., Mehta, S. B., & Kleinfeld, D. (2011). Quality Metrics to Accompany Spike Sorting of Extracellular Signals. *Journal of
557 Neuroscience*, 31(24), 8699–8705. doi: 10.1523/JNEUROSCI.0971-11.2011
- 558 Holland, P. C. (1992). Occasion setting in pavlovian conditioning. *Psychology of Learning and Motivation*, 28(C), 69–125. doi:
559 10.1016/S0079-7421(08)60488-0
- 560 Hollerman, J. R., Tremblay, L., & Schultz, W. (1998). Influence of Reward Expectation on Behavior-Related Neuronal Activity in
561 Primate Striatum. *Journal of Neurophysiology*, 80(2), 947–963. doi: 10.1152/jn.1998.80.2.947
- 562 Honey, R. C., Iordanova, M. D., & Good, M. (2014). Associative structures in animal learning: Dissociating elemental and
563 configural processes. *Neurobiology of Learning and Memory*, 108, 96–103. doi: 10.1016/j.nlm.2013.06.002
- 564 Hyman, S. E., Malenka, R. C., & Nestler, E. J. (2006). NEURAL MECHANISMS OF ADDICTION: The Role of Reward-Related
565 Learning and Memory. *Annual Review of Neuroscience*, 29(1), 565–598. doi: 10.1146/annurev.neuro.29.051605.113009
- 566 Ikemoto, S. (2007). Dopamine reward circuitry: Two projection systems from the ventral midbrain to the nucleus accumbens-
567 olfactory tubercle complex. *Brain Research Reviews*, 56(1), 27–78. doi: 10.1016/j.brainresrev.2007.05.004
- 568 Ishikawa, A., Ambroggi, F., Nicola, S. M., & Fields, H. L. (2008). Dorsomedial Prefrontal Cortex Contribution to Behav-
569 ioral and Nucleus Accumbens Neuronal Responses to Incentive Cues. *Journal of Neuroscience*, 28(19), 5088–5098. doi:
570 10.1523/JNEUROSCI.0253-08.2008
- 571 Joel, D., Niv, Y., & Ruppin, E. (2002). Actor-critic models of the basal ganglia: new anatomical and computational perspectives.
572 *Neural Networks*, 15(4-6), 535–547. doi: 10.1016/S0893-6080(02)00047-3
- 573 Kaczkurkin, A. N., Burton, P. C., Chazin, S. M., Manbeck, A. B., Espensen-Sturges, T., Cooper, S. E., ... Lissek, S. (2017).
574 Neural substrates of overgeneralized conditioned fear in PTSD. *American Journal of Psychiatry*, 174(2), 125–134. doi:
575 10.1176/appi.ajp.2016.15121549
- 576 Kaczkurkin, A. N., & Lissek, S. (2013). Generalization of Conditioned Fear and Obsessive-Compulsive Traits. *Journal of Psychol-
577 ogy & Psychotherapy*, 7, 3. doi: 10.4172/2161-0487.S7-003
- 578 Kalivas, P. W., & Volkow, N. D. (2005). The neural basis of addiction: A pathology of motivation and choice. *American Journal of
579 Psychiatry*, 162(8), 1403–1413. doi: 10.1176/appi.ajp.162.8.1403
- 580 Kapur, S. (2003). Psychosis as a state of aberrant salience: A framework linking biology, phenomenology, and pharmacology in
581 schizophrenia. *American Journal of Psychiatry*, 160(1), 13–23. doi: 10.1176/appi.ajp.160.1.13

- 582 Khamassi, M., & Humphries, M. D. (2012). Integrating cortico-limbic-basal ganglia architectures for learning model-based and
583 model-free navigation strategies. *Frontiers in Behavioral Neuroscience*, 6, 79. doi: 10.3389/fnbeh.2012.00079
- 584 Khamassi, M., Mulder, A. B., Tabuchi, E., Douchamps, V., & Wiener, S. I. (2008). Anticipatory reward signals in ventral striatal
585 neurons of behaving rats. *European Journal of Neuroscience*, 28(9), 1849–1866. doi: 10.1111/j.1460-9568.2008.06480.x
- 586 Lansink, C. S., Goltstein, P. M., Lankelma, J. V., Joosten, R. N. J. M. A., McNaughton, B. L., & Pennartz, C. M. A. (2008).
587 Preferential Reactivation of Motivationally Relevant Information in the Ventral Striatum. *Journal of Neuroscience*, 28(25),
588 6372–6382. doi: 10.1523/JNEUROSCI.1054-08.2008
- 589 Lansink, C. S., Goltstein, P. M., Lankelma, J. V., McNaughton, B. L., & Pennartz, C. M. (2009). Hippocampus leads ventral
590 striatum in replay of place-reward information. *PLoS Biology*, 7(8), e1000173. doi: 10.1371/journal.pbio.1000173
- 591 Lansink, C. S., Jackson, J. C., Lankelma, J. V., Ito, R., Robbins, T. W., Everitt, B. J., & Pennartz, C. M. A. (2012). Reward Cues
592 in Space: Commonalities and Differences in Neural Coding by Hippocampal and Ventral Striatal Ensembles. *Journal of*
593 *Neuroscience*, 32(36), 12444–12459. doi: 10.1523/JNEUROSCI.0593-12.2012
- 594 Lansink, C. S., Meijer, G. T., Lankelma, J. V., Vinck, M. A., Jackson, J. C., & Pennartz, C. M. A. (2016). Reward Expectancy
595 Strengthens CA1 Theta and Beta Band Synchronization and Hippocampal-Ventral Striatal Coupling. *Journal of Neuro-*
596 *science*, 36(41), 10598–10610. doi: 10.1523/JNEUROSCI.0682-16.2016
- 597 Lavoie, A. M., & Mizumori, S. J. (1994). Spatial, movement- and reward-sensitive discharge by medial ventral striatum neurons of
598 rats. *Brain Research*, 638(1-2), 157–168. doi: 10.1016/0006-8993(94)90645-9
- 599 Lee, D., Seo, H., & Jung, M. W. (2012). Neural Basis of Reinforcement Learning and Decision Making. *Annual Review of*
600 *Neuroscience*, 35(1), 287–308. doi: 10.1146/annurev-neuro-062111-150512
- 601 Lissek, S., Kaczkurkin, A. N., Rabin, S., Geraci, M., Pine, D. S., & Grillon, C. (2014). Generalized anxiety disor-
602 der is associated with overgeneralization of classically conditioned fear. *Biological Psychiatry*, 75(11), 909–915. doi:
603 10.1016/j.biopsych.2013.07.025
- 604 Maia, T. V. (2009). Reinforcement learning, conditioning, and the brain: Successes and challenges. *Cognitive, Affective and*
605 *Behavioral Neuroscience*, 9(4), 343–364. doi: 10.3758/CABN.9.4.343
- 606 Maia, T. V., & Frank, M. J. (2011). From reinforcement learning models to psychiatric and neurological disorders. *Nature*
607 *Neuroscience*, 14(2), 154–162. doi: 10.1038/nn.2723
- 608 Malhotra, S., Cross, R. W., Zhang, A., & van der Meer, M. A. A. (2015). Ventral striatal gamma oscillations are highly variable
609 from trial to trial, and are dominated by behavioural state, and only weakly influenced by outcome value. *European Journal*
610 *of Neuroscience*, 42(10), 2818–2832. doi: 10.1038/nn.2723
- 611 McDannald, M. A., Lucantonio, F., Burke, K. A., Niv, Y., & Schoenbaum, G. (2011). Ventral Striatum and Orbitofrontal Cortex
612 Are Both Required for Model-Based, But Not Model-Free, Reinforcement Learning. *Journal of Neuroscience*, 31(7), 2700–
613 2705. doi: 10.1523/JNEUROSCI.5499-10.2011
- 614 McGinty, V. B., Lardeux, S., Taha, S. A., Kim, J. J., & Nicola, S. M. (2013). Invigoration of reward seeking by cue and proximity

- 615 encoding in the nucleus accumbens. *Neuron*, 78(5), 910–922. doi: 10.1016/j.neuron.2013.04.010
- 616 Mulder, A. B., Shibata, R., Trullier, O., & Wiener, S. I. (2005). Spatially selective reward site responses in tonically active neurons
617 of the nucleus accumbens in behaving rats. *Experimental Brain Research*, 163(1), 32–43. doi: 10.1007/s00221-004-2135-3
- 618 Mulder, A. B., Tabuchi, E., & Wiener, S. I. (2004). Neurons in hippocampal afferent zones of rat striatum parse routes into
619 multi-pace segments during maze navigation. *European Journal of Neuroscience*, 19(7), 1923–1932. doi: 10.1111/j.1460-
620 9568.2004.03301.x
- 621 Nicola, S. M. (2004). Cue-Evoked Firing of Nucleus Accumbens Neurons Encodes Motivational Significance During a Discrimi-
622 native Stimulus Task. *Journal of Neurophysiology*, 91(4), 1840–1865. doi: 10.1152/jn.00657.2003
- 623 Nicola, S. M. (2010). The Flexible Approach Hypothesis: Unification of Effort and Cue-Responding Hypotheses for the Role of
624 Nucleus Accumbens Dopamine in the Activation of Reward-Seeking Behavior. *Journal of Neuroscience*, 30(49), 16585–
625 16600. doi: 10.1523/JNEUROSCI.3958-10.2010
- 626 Niv, Y., Daw, N. D., Joel, D., & Dayan, P. (2007). Tonic dopamine: Opportunity costs and the control of response vigor. *Psy-
627 chopharmacology*, 191(3), 507–520. doi: 10.1007/s00213-006-0502-4
- 628 Noonan, M. P., Chau, B. K., Rushworth, M. F., & Fellows, L. K. (2017). Contrasting Effects of Medial and Lateral Orbitofrontal
629 Cortex Lesions on Credit Assignment and Decision-Making in Humans. *The Journal of Neuroscience*, 37(29), 7023–7035.
630 doi: 10.1523/JNEUROSCI.0692-17.2017
- 631 Paxinos, G., & Watson, C. (1998). *The Rat Brain in Stereotaxic Coordinates* (4th ed.). San Diego: Academic Press. doi:
632 10.1523/JNEUROSCI.0692-17.2017
- 633 Pennartz, C. M. A. (2004). The Ventral Striatum in Off-Line Processing: Ensemble Reactivation during Sleep and Modulation by
634 Hippocampal Ripples. *Journal of Neuroscience*, 24(29), 6446–6456. doi: 10.1523/JNEUROSCI.0575-04.2004
- 635 Rescorla, R. A., & Solomon, R. L. (1967). Two-Process Learning Theory: Relationships Between Pavlovian Conditioning and
636 Instrumental Learning. *Psychological Review*, 74(3), 151–182. doi: 10.1037/h0024475
- 637 Robinson, T. E., & Flagel, S. B. (2009). Dissociating the Predictive and Incentive Motivational Properties of Reward-Related Cues
638 Through the Study of Individual Differences. *Biological Psychiatry*, 65(10), 869–873. doi: 10.1016/j.biopsych.2008.09.006
- 639 Roesch, M. R., Singh, T., Brown, P. L., Mullins, S. E., & Schoenbaum, G. (2009). Ventral Striatal Neurons Encode the Value
640 of the Chosen Action in Rats Deciding between Differently Delayed or Sized Rewards. *Journal of Neuroscience*, 29(42),
641 13365–13376. doi: 10.1523/JNEUROSCI.2572-09.2009
- 642 Roitman, M. F., Wheeler, R. A., & Carelli, R. M. (2005). Nucleus accumbens neurons are innately tuned for reward-
643 ing and aversive taste stimuli, encode their predictors, and are linked to motor output. *Neuron*, 45(4), 587–597. doi:
644 10.1016/j.neuron.2004.12.055
- 645 Saddoris, M. P., Stamatakis, A., & Carelli, R. M. (2011). Neural correlates of Pavlovian-to-instrumental transfer in the nucleus ac-
646 cumbens shell are selectively potentiated following cocaine self-administration. *European Journal of Neuroscience*, 33(12),
647 2274–2287. doi: 10.1111/j.1460-9568.2011.07683.x

- 648 Salamone, J. D., & Correa, M. (2012). The Mysterious Motivational Functions of Mesolimbic Dopamine. *Neuron*, 76(3), 470–485.
649 doi: 10.1016/j.neuron.2012.10.021
- 650 Schultz, W. (2016). Dopamine reward prediction error coding. *Dialogues in Clinical Neuroscience*, 18(1), 23–32. doi:
651 10.1038/nrn.2015.26
- 652 Schultz, W., Dayan, P., & Montague, P. R. (1997). A neural substrate of prediction and reward. *Science*, 275(5306), 1593–1599.
653 doi: 10.1126/science.275.5306.1593
- 654 Setlow, B., Schoenbaum, G., & Gallagher, M. (2003). Neural encoding in ventral striatum during olfactory discrimination learning.
655 *Neuron*, 38(4), 625–636. doi: 10.1016/S0896-6273(03)00264-2
- 656 Shidara, M., Aigner, T. G., & Richmond, B. J. (1998). Neuronal signals in the monkey ventral striatum related to progress through
657 a predictable series of trials. *Journal of Neuroscience*, 18(7), 2613–25. doi: 10.1016/S0896-6273(03)00264-2
- 658 Sjulson, L., Peyrache, A., Cumpelik, A., Cassataro, D., & Buszaki, G. (2017). Cocaine place conditioning strengthens location-
659 specific hippocampal inputs to the nucleus accumbens. *bioRxiv*, 1–10. doi: 10.1101/105890
- 660 Sleezer, B. J., Castagno, M. D., & Hayden, B. Y. (2016). Rule Encoding in Orbitofrontal Cortex and Striatum Guides Selection.
661 *Journal of Neuroscience*, 36(44), 11223–11237. doi: 10.1523/JNEUROSCI.1766-16.2016
- 662 Strait, C. E., Sleezer, B. J., Blanchard, T. C., Azab, H., Castagno, M. D., & Hayden, B. Y. (2016). Neuronal selectivity
663 for spatial positions of offers and choices in five reward regions. *Journal of Neurophysiology*, 115(3), 1098–1111. doi:
664 10.1152/jn.00325.2015
- 665 Sugam, J. A., Saddoris, M. P., & Carelli, R. M. (2014). Nucleus accumbens neurons track behavioral preferences and reward
666 outcomes during risky decision making. *Biological Psychiatry*, 75(10), 807–816. doi: 10.1016/j.biopsych.2013.09.010
- 667 Sutton, R., & Barto, A. (1998). *Reinforcement Learning: An Introduction* (Vol. 9) (No. 5). MIT Press, Cambridge, MA. doi:
668 10.1109/TNN.1998.712192
- 669 Tabuchi, E. T., Mulder, A. B., & Wiener, S. I. (2000). Position and behavioral modulation of synchronization of hippocam-
670 pal and accumbens neuronal discharges in freely moving rats. *Hippocampus*, 10(6), 717–728. doi: 10.1002/1098-
671 1063(2000)10:6;717::AID-HIPO1009;3.0.CO;2-3
- 672 Takahashi, Y. K., Langdon, A. J., Niv, Y., & Schoenbaum, G. (2016). Temporal Specificity of Reward Prediction Errors
673 Signaled by Putative Dopamine Neurons in Rat VTA Depends on Ventral Striatum. *Neuron*, 91(1), 182–193. doi:
674 10.1016/j.neuron.2016.05.015
- 675 van der Meer, M. A. A., & Redish, A. D. (2011). Theta Phase Precession in Rat Ventral Striatum Links Place and Reward
676 Information. *Journal of Neuroscience*, 31(8), 2843–2854. doi: 10.1523/JNEUROSCI.4869-10.2011
- 677 West, E. A., & Carelli, R. M. (2016). Nucleus Accumbens Core and Shell Differentially Encode Reward-Associated Cues after
678 Reinforcer Devaluation. *Journal of Neuroscience*, 36(4), 1128–1139. doi: 10.1523/JNEUROSCI.2976-15.2016
- 679 Wiener, S. I., Shibata, R., Tabuchi, E., Trullier, O., Albertin, S. V., & Mulder, A. B. (2003). Spatial and behavioral correlates in
680 nucleus accumbens neurons in zones receiving hippocampal or prefrontal cortical inputs. *International Congress Series*,

681 *I250(C)*, 275–292. doi: 10.1016/S0531-5131(03)00978-6

682 Yun, I. A., Wakabayashi, K. T., Fields, H. L., & Nicola, S. M. (2004). The Ventral Tegmental Area Is Required for the Behavioral
683 and Nucleus Accumbens Neuronal Firing Responses to Incentive Cues. *Journal of Neuroscience*, 24(12), 2923–2933. doi:
684 10.1523/JNEUROSCI.5282-03.2004

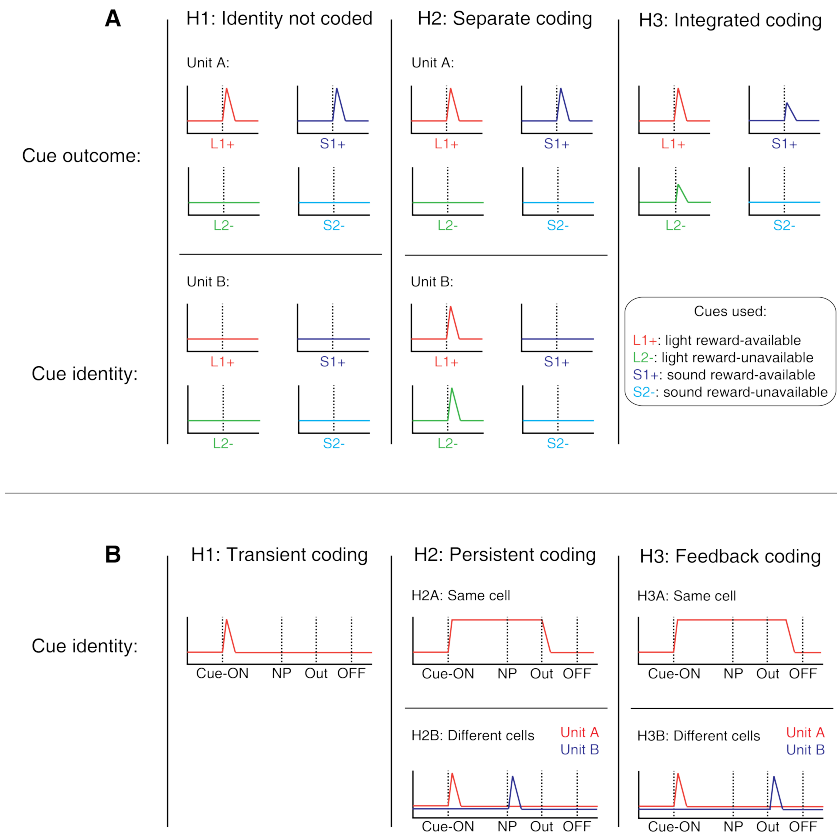


Figure 1: Schematic of potential coding strategies for cue identity (light, sound) and cue outcome (reward-available, reward-unavailable) employed by single units in the NAc across different units (A) and in time (B). **A:** Displayed are schematic PETHs illustrating putative responses to different cues under different hypotheses of how cue identity and outcome are coded. H1 (left panel): Coding of cue identity is absent in the NAc. Top: Unit A encodes a motivationally relevant variable, such as expected outcome, similarly across other cue features, such as cue identity or physical location. Hypothetical plot is firing rate across time. L1+ (red) signifies a reward-available light cue, S1+ (navy blue) a reward-available sound cue, L2- (green) a reward-unavailable light cue, S2- (light blue) a reward-unavailable sound cue. Dashed line indicates onset of cue. Bottom: No units within the NAc discriminate their firing according to cue identity. H2 (middle panel): Coding of cue identity occurs independently of encoding of motivationally relevant variables such as expected outcome or subsequent vigor. Top: Same as H1, with unit A discriminating between reward-available and reward-unavailable cues. Bottom: Unit B discriminates firing across stimulus modalities, depicted here as firing to light cues but not sound cues. H3 (right panel): Coding of cue identity is integrated with coding of other motivationally relevant variables. Hypothetical example demonstrating a unit that responds to outcome-predictive cues, but firing rate is also modulated by cue identity, firing most for the reward-available light cue. **B:** Displayed are schematic PETHs illustrating potential ways in which cue identity signals may persist over time. H1 (left panel): Cue-onset triggers a transient response to a unit that codes for cue identity. Dashed lines indicate time of a behavioral or environmental event. 'Cue-ON' signifies onset of cue, 'NP' signifies when the rat holds a nosepoke at a reward receptacle, 'Out' signifies when the outcome is revealed, 'OFF' signifies when the cue turns off. H2 (middle panel): Coding of cue identity persists during a nosepoke hold period until outcome is revealed. Coding can either be maintained by the same unit as during cue-onset (H2A) or by a sequence of units (H2B). H3 (right panel): Coding of cue identity persists after the outcome is received when the rat gets feedback about his decision, by either the same unit as during cue-onset (H3A) or by a sequence of units (H3B). The same hypotheses apply to other information-containing aspects of the environment when the cue is presented, such as the physical location of the cue.

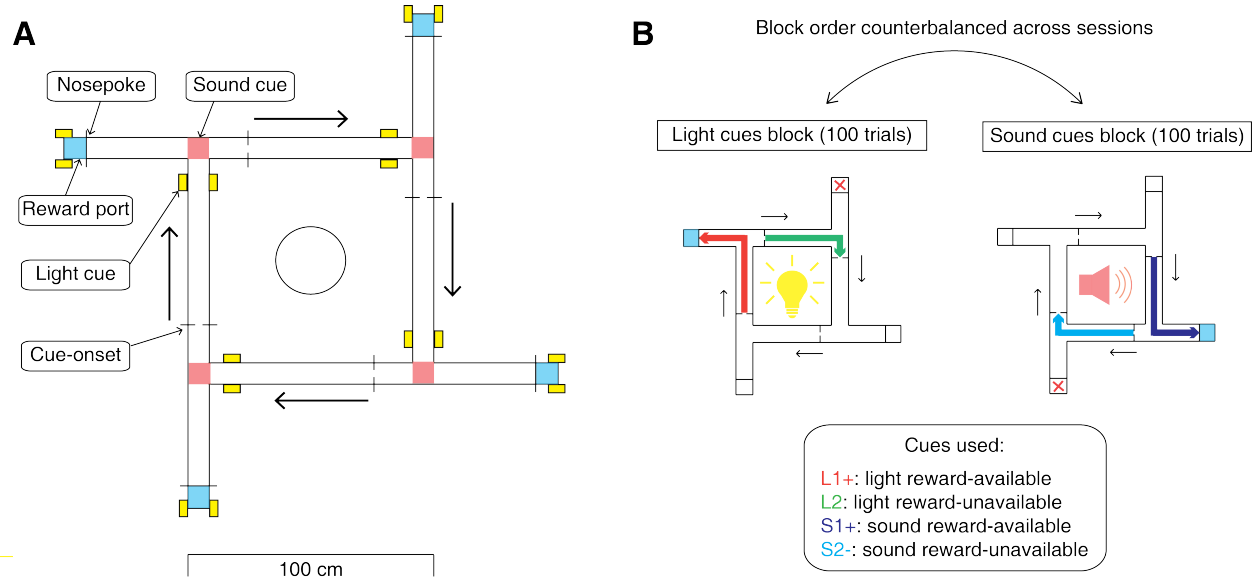


Figure 2: Schematic of behavioral task. **A:** To scale depiction of square track consisting of multiple identical T-choice points. At each choice point, the availability of 12% sucrose reward at the nearest reward receptacle (light blue fill) was signaled by one of four possible cues, presented when the rat initiated a trial by crossing a photobeam on the track (dashed lines). Photobeams at the ends of the arms by the receptacles registered Nosepokes (solid lines). Rectangular boxes with yellow fill indicate location of LEDs used for light cues. Speakers for tone cues were placed underneath the choice points, indicated by magenta fill on track. Arrows outside of track indicate correct running direction. Circle in the center indicates location of pedestal during pre- and post-records. Scale bar is located beneath the track. **B:** Progression of a recording session. A session was started with a 5 minute recording period on a pedestal placed in the center of the apparatus. Rats then performed the light and sound blocks of the cue discrimination task in succession for 100 trials each, followed by another 5 minute recording period on the pedestal. Left in figure depicts a light block, showing an example trajectory for a correct reward-available (approach trial; red) and reward-unavailable (skip trial; green) trial. Right in figure depicts a sound block, with a reward-available (approach trial; navy blue) and reward-unavailable (skip trial; light blue) trial. Ordering of the light and sound blocks was counterbalanced across sessions. Reward-available and reward-unavailable cues were presented pseudo-randomly, such that not more than two of the same type of cue could be presented in a row. Location of the cue on the track was irrelevant for behavior, all cue locations contained an equal amount of reward-available and reward-unavailable trials.

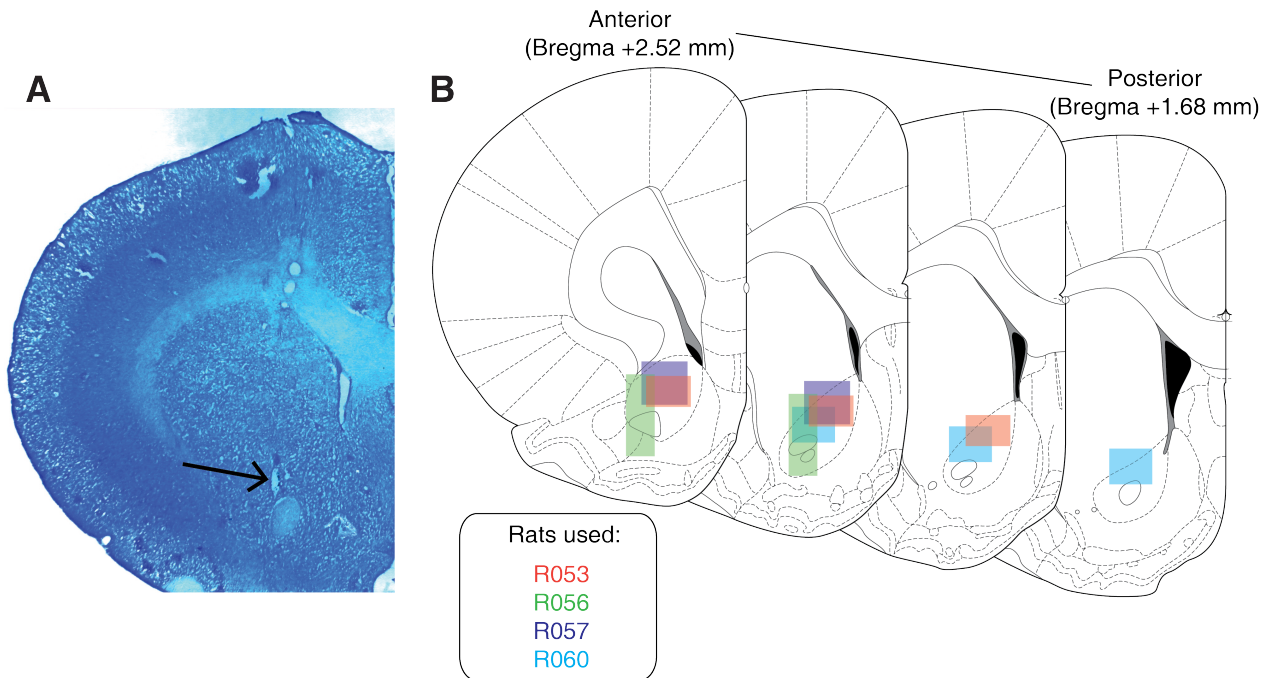


Figure 3: Histological verification of recording sites. Upon completion of experiments, brains were sectioned and tetrode placement was confirmed. **A:** Example section from R060 showing a recording site in the NAc core just dorsal to the anterior commissure (arrow). **B:** Schematic showing recording areas for all subjects.

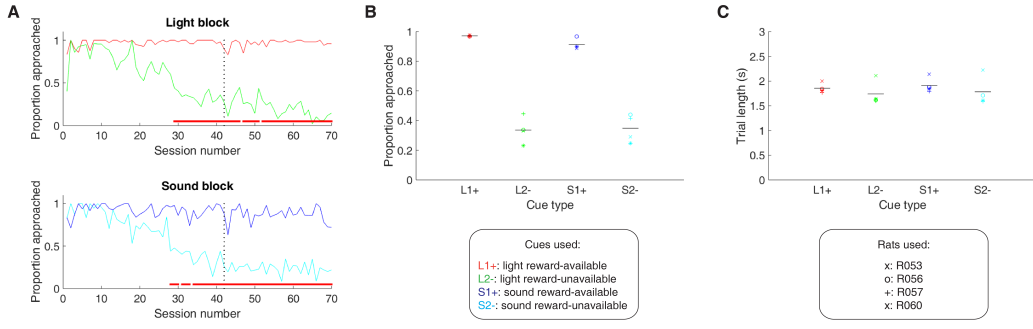


Figure 4: Performance on the behavioral task. **A.** Example learning curves across sessions from a single subject (R060) showing the proportion approached for reward-available (red line for light block, navy blue line for sound block) and reward-unavailable trials (green line for light block, light blue line for sound block) for light (top) and sound (bottom) blocks. Fully correct performance corresponds to an approach proportion of 1 for reward-available trials and 0 for reward-unavailable trials. Rats initially approach on both reward-available and reward-unavailable trials, and learn with experience to skip non-rewarded trials. Red bars indicate days in which a rat statistically discriminated between reward-available and reward-unavailable cues, determined by a chi square test. Dashed line indicates time of electrode implant surgery. **B-C:** Summary of performance during recording sessions for each rat. **B:** Proportion approached for all rats, averaged across all recording sessions. Different columns indicate the different cues (reward-available (red) and reward-unavailable (green) light cues, reward-available (navy blue) and reward-unavailable (light blue) sound cues). Different symbols correspond to individual subjects; horizontal black line shows the mean. All rats learned to discriminate between reward-available and reward-unavailable cues, as indicated by the clear difference of proportion approached between reward-available (~90% approached) and reward-unavailable cues (~30% approached), for both blocks (see Results for statistics). **C:** Average trial length for each cue. Note that the time to complete a trial was comparable for the different cues.

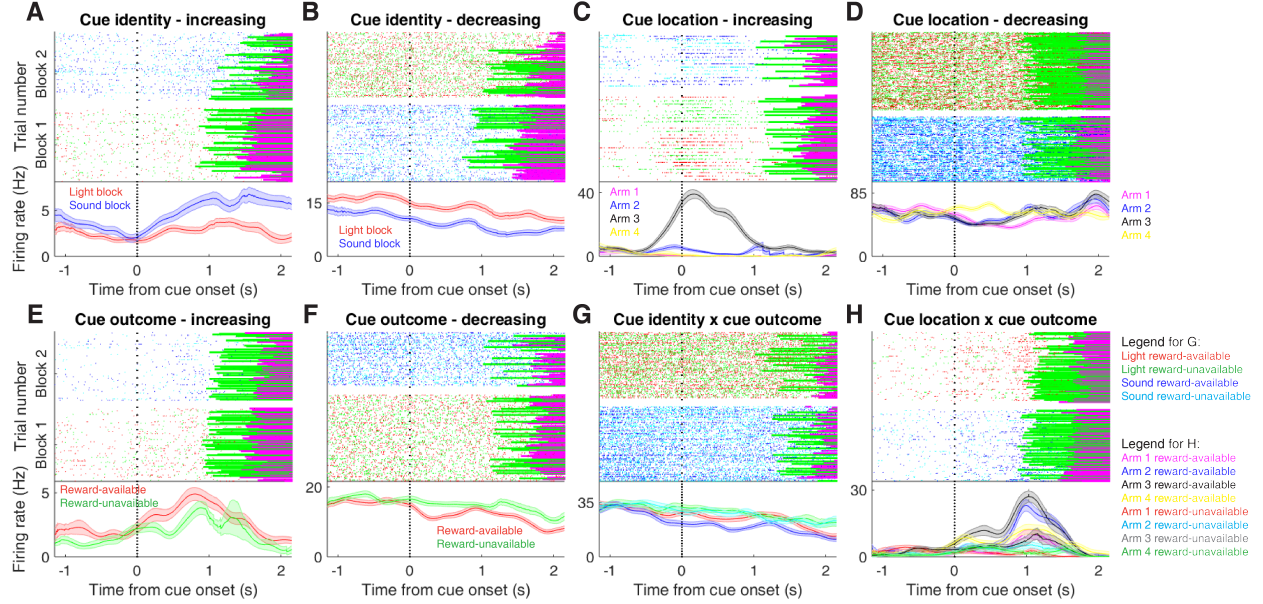


Figure 5: Examples of different cue-modulated NAc units influenced by various task parameters. **A:** Example of a cue-modulated NAc unit that showed an increase in firing following the cue, and encoded cue identity. Top: rasterplot showing the spiking activity across all trials aligned to cue-onset. Spikes across trials are color-coded according to cue type (red: reward-available light; green: reward-unavailable light; navy blue: reward-available sound; light blue: reward-unavailable sound). Green and magenta bars indicate trial termination when a rat initiated the next trial or made a nosepoke, respectively. White space halfway up the rasterplot indicates switching from one block to the next. Dashed line indicates cue onset. Bottom: PETHs showing the average smoothed firing rate for the unit for trials during light (red) and sound (blue) blocks, aligned to cue-onset. Lightly shaded area indicates standard error of the mean. Note this unit showed a larger increase in firing to sound cues. **B:** An example of a unit that was responsive to cue identity as in A, but for a unit that showed a decrease in firing to the cue. Note the sustained higher firing rate during the light block. **C-D:** Cue-modulated units that encoded cue location, each color in the PETHs represents average firing response for a different cue location. **C:** The firing rate of this unit only changed on arm 3 of the task. **D:** Firing decreased for this unit on all arms but arm 4. **E-F:** Cue-modulated units that encoded cue outcome, with the PETHs comparing reward-available (red) and reward-unavailable (green) trials. **E:** This unit showed a slightly higher response during presentation of reward-available cues. **F:** This unit showed a dip in firing when presented with reward-available cues. **G-H:** Examples of cue-modulated units that encoded multiple cue features. **G:** This unit integrated cue identity and outcome. **H:** An example of a unit that integrated cue identity and location.

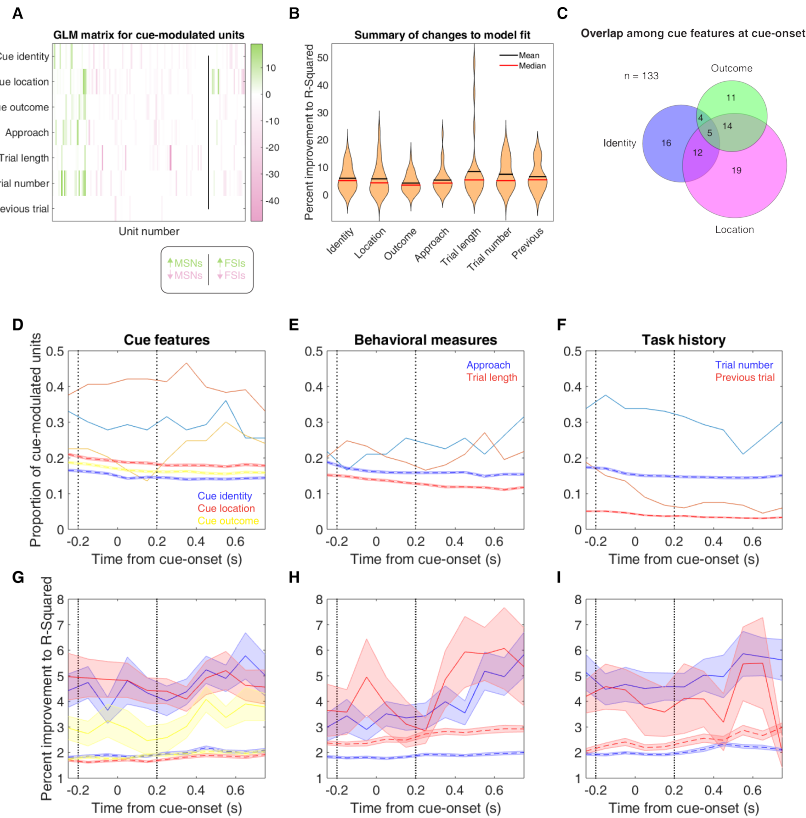


Figure 6: Summary of influence of various task parameters on cue-modulated NAc units after cue-onset. **A:** GLM matrix illustrating the contribution of various task parameters to NAc unit firing rates. A stepwise GLM was fit to each unit that showed evidence of cue modulation by a Wilcoxon signed-rank test. Each row represents a given task parameter, and each column corresponds to a single unit. Colors indicate how much of the firing rate variance an individual predictor contributed to the model, as measured by differences in R-squared between the final model and the model minus the predictor of interest. Ordering from left to right: MSNs that increased firing in response to the cue (green, left of line), MSNs with a decreasing response (red, left of line), FSIs with an increasing response (green, right of line), FSIs with a decreasing response (red, right of line). Darker shades indicate more firing rate variance explained by a given predictor. Black line indicates separation of MSNs and FSIs. Scale bar indicates range of improvements to model fit for units with an increasing (green) and decreasing (red) response to the cue. **B:** Violin plots demonstrating changes in R-squared values with the addition of each of the individual predictors. The mean, median, and distribution of changes in R-squared values is plotted for each of the seven task parameters used in the GLM. **C:** Venn diagram illustrating the number of cue-modulated units encoding cue identity (blue circle), cue location (green circle), cue outcome (pink circle), as well as the overlap among units that encoded multiple cue features. **D-F:** Sliding window GLM illustrating the proportion of cue-modulated units influenced by various predictors around time of cue-onset. **D:** Sliding window GLM (bin size: 500 ms; step size: 100 ms) demonstrating the proportion of cue-modulated units where cue identity (blue solid line), cue location (red solid line), and cue outcome (yellow solid line) significantly contributed to the model at various time epochs relative to cue-onset. Dashed colored lines indicate the average of shuffling the firing rate order that went into the GLM 100 times. Points in between the two vertical dashed lines indicate bins where both pre- and post-cue-onset time periods were used in the GLM. **E:** Same as D, but for approach behavior and trial length. **F:** Same as D, but for trial number³⁶ and previous trial. **G-I:** Average improvement to model fit. **G:** Average percent improvement to R-squared for units where cue identity, cue location, or cue outcome were significant contributors to the final model for time epochs surrounding cue onset. Shaded area around mean represents the standard error of the mean. **H:** Same as G, but for approach behavior and trial length. **I:** Same G, but for trial number and previous trial.

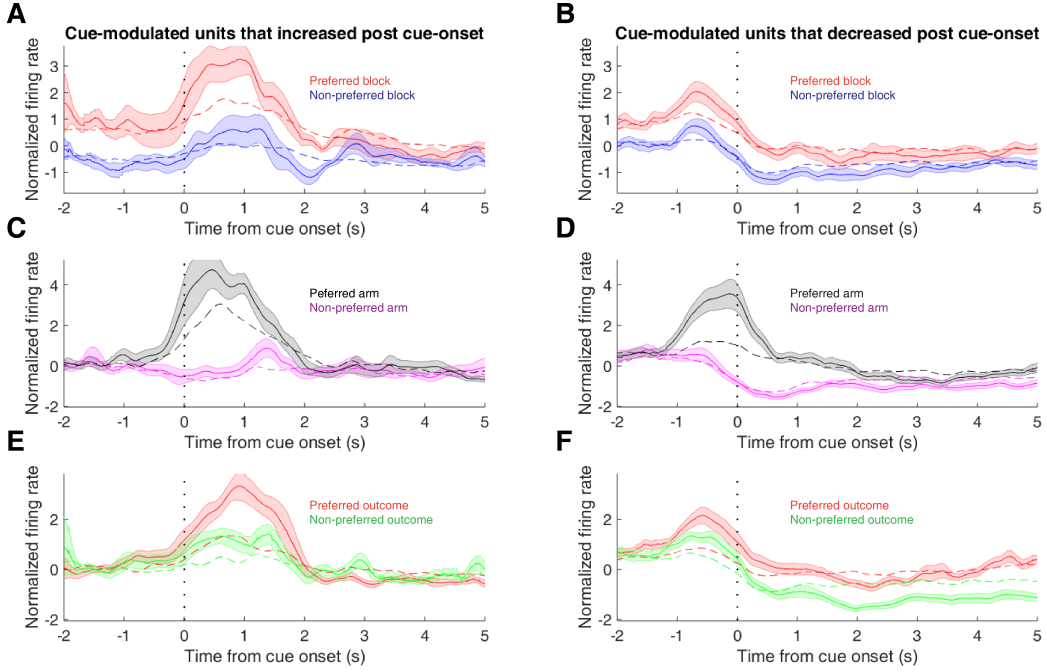


Figure 7: Population-level averages of cue feature sensitive NAc units. **A:** Average smoothed normalized (z-score) activity for cue-modulated units where cue identity was a significant predictor in the GLM, aligned to cue-onset. Activity is plotted for preferred stimulus block (red) and non-preferred stimulus block (blue). Dashed vertical line indicates onset of cue. Dashed color lines indicate the result of shuffling the identity of the units used for this average 1000 times. Lightly shaded area indicates standard error of the mean. Note larger increase to preferred stimulus block over nonpreferred stimulus block. Black lines indicate the average of 1000 rounds of random sampling of units from the non-drifting population for the preferred and non-preferred blocks. **B:** Same as A but for units that decreased in response to cue. Note population level activity reveals units classified as decreasing in response to cue show a biphasic response at the population level, with a transient increase around the time the rat starts on the arm, followed by a minimum after cue onset. Also, note the sustained difference in firing between the two blocks. **C-D:** Same as A-B for cue location. Activity is plotted for most preferred arm (black) and least preferred arm (magenta). **E-F:** Same as A-B for cue outcome. Activity is plotted for preferred expected outcome (red), and nonpreferred outcome (green). Note the larger increase to the cue representing the units preferred outcome (E), and the sustained decrease to the nonpreferred outcome (F).

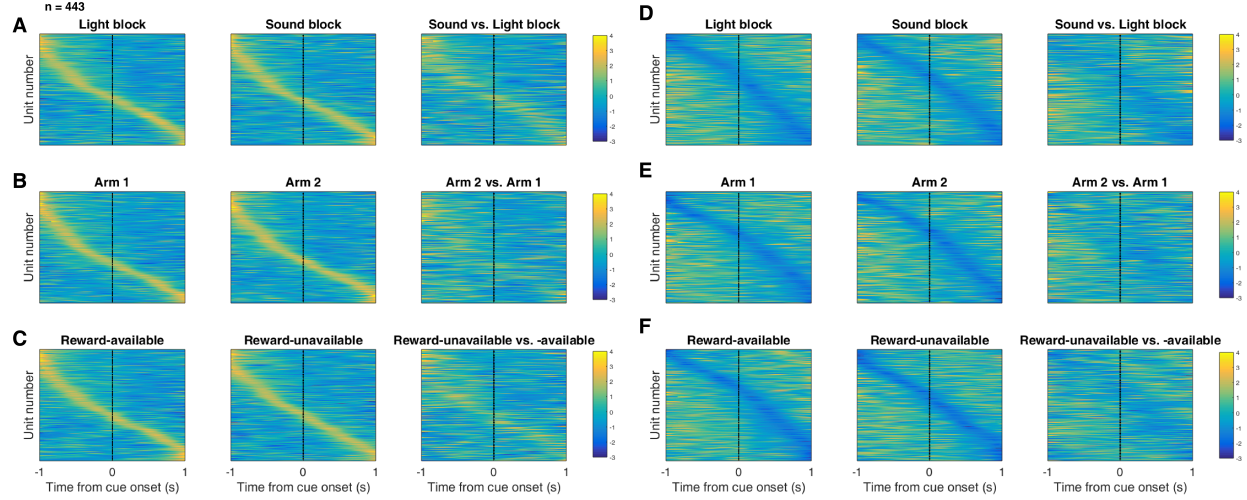


Figure 8: Distribution of NAc firing rates across time surrounding cue onset. Each panel shows normalized (z-score) firing rates for all recorded NAc units (each row corresponds to one unit) as a function of time (time 0 indicates cue onset), averaged across all trials for a specific cue type, indicated by text labels. **A-C:** Heat plots aligned to normalized peak firing rates. **A, left:** Heat plot showing smoothed normalized firing activity of all recorded NAc units ordered according to the time of their peak firing rate during the light block. Each row is a units average activity across time to the light block. Dashed line indicates cue onset. Notice the yellow band across time, indicating all aspects of visualized task space were captured by the peak firing rates of various units. **A, middle:** Same units ordered according to the time of the peak firing rate during the sound block. Note that for both blocks, units tile time approximately uniformly with a clear diagonal of elevated firing rates. **A, right:** Unit firing rates taken from the sound block, ordered according to peak firing rate taken from the light block. Note that a weaker but still discernible diagonal persists, indicating partial similarity between firing rates in the two blocks. A similar pattern exists for within-block comparisons suggesting that reordering any two sets of trials produces this partial similarity, however correlations within blocks are more similar than correlations across blocks (see text). **B:** Same layout as in A, except that the panels now compare two different locations on the track instead of two cue modalities. As for the different cue modalities, NAc units clearly discriminate between locations, but also maintain some similarity across locations, as evident from the visible diagonal in the right panel. Two example locations were used for display purposes; other location pairs showed a similar pattern. **C:** Same layout as in A, except that panels now compare reward-available and reward-unavailable trials. **D-F:** Heat plots aligned to normalized minimum firing rates. **D:** Responses during different stimulus blocks as in A, but with units ordered according to the time of their minimum firing rate. **E:** Responses during trials on different arms as in B, but with units ordered by their minimum firing rate. **F:** Responses during cues signalling different outcomes as in C, but with units ordered by their minimum firing rate. Overall, NAc units “tiled” experience on the task, as opposed to being confined to specific task events only. Units from all sessions and animals were pooled for this analysis.

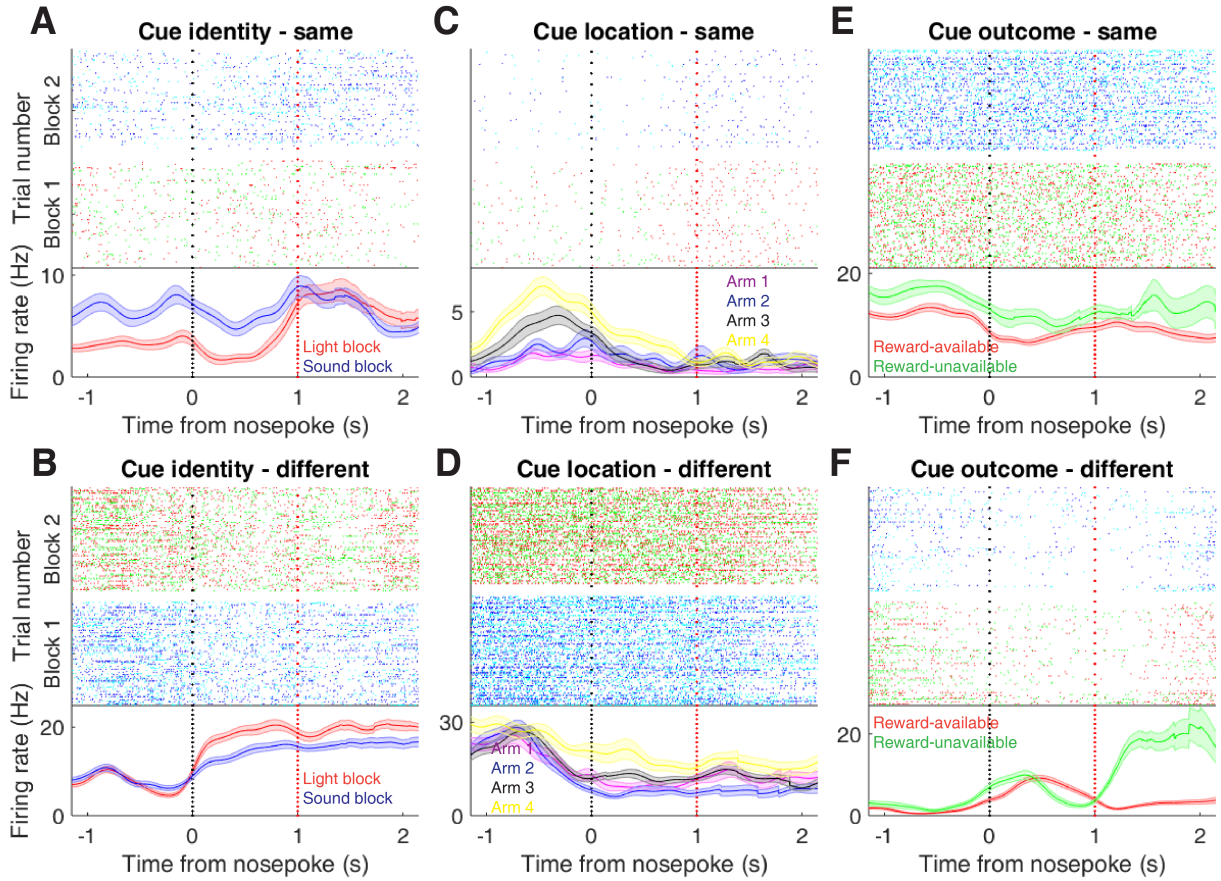


Figure 9: Examples of cue-modulated NAc units influenced by various task parameters at time of nosepoke. **A:** Example of a cue-modulated NAc unit that encoded cue identity at both cue-onset and during nosepoke hold. Top: rasterplot showing the spiking activity across all trials aligned to nosepoke. Spikes across trials are color coded according to cue type (red: reward-available light; green: reward-unavailable light; navy blue: reward-available sound; light blue: reward-unavailable sound). White space halfway up the rasterplot indicates switching from one block to the next. Black dashed line indicates nosepoke. Red dashed line indicates receipt of outcome. Bottom: PETHs showing the average smoothed firing rate for the unit for trials during light (red) and sound (blue) blocks, aligned to nosepoke. Lightly shaded area indicates standard error of the mean. Note this unit showed a sustained increase in firing to sound cues during the trial. **B:** An example of a unit that was responsive to cue identity at time of nosepoke but not cue-onset. **C-D:** Cue-modulated units that encoded cue location, at both cue-onset and nosepoke (C), and only nosepoke (D). Each color in the PETHs represents average firing response for a different cue location. **E-F:** Cue-modulated units that encoded cue outcome, at both cue-onset and nosepoke (E), and only nosepoke (F), with the PETHs comparing reward-available (red) and reward-unavailable (green) trials.

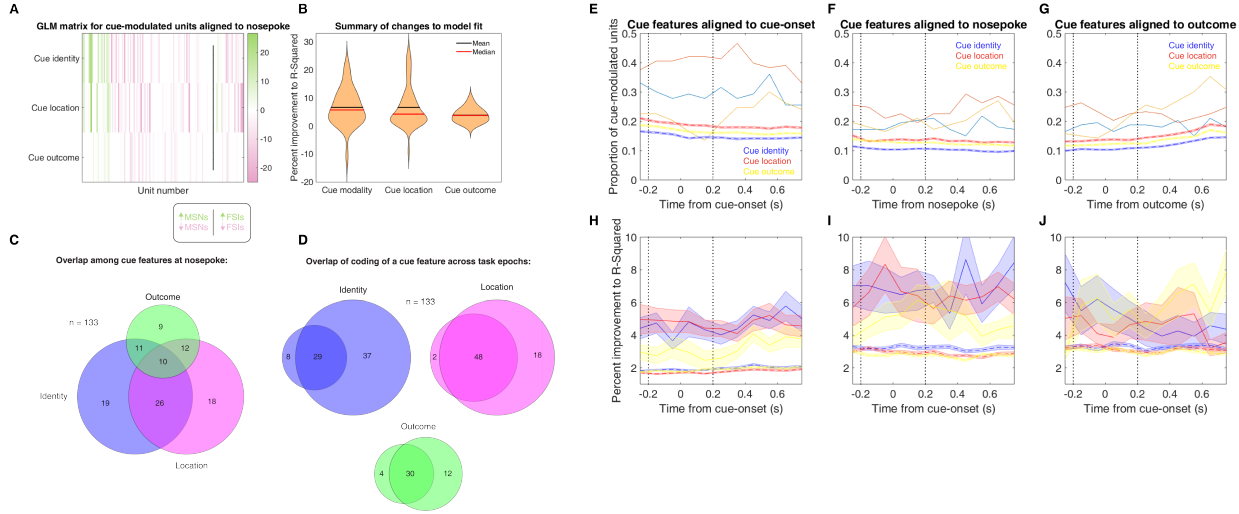


Figure 10: Summary of influence of various task parameters of cue-modulated NAc units during nosepoke. **A:** GLM matrix illustrating the contribution of various task parameters to NAc unit firing rates. A stepwise GLM was fit to each unit that showed evidence of cue modulation by a Wilcoxon signed-rank test. Each row represents a given task parameter, and each column corresponds to a single unit. Colors indicate how much of the firing rate variance an individual predictor contributed to the model, as measured by differences in R-squared between the final model and the model minus the predictor of Interest. Ordering from left to right: MSNs that increased firing in response to the cue (green, left of line), MSNs with a decreasing response (red, left of line), FSIs with an increasing response (green, right of line), FSIs with a decreasing response (red, right of line). Darker shades indicate more firing rate variance explained by a given predictor. Black line indicates separation of MSNs and FSIs. **B:** Violin plots demonstrating changes in R-squared values with the addition of each of the individual predictors. The mean, median, and distribution of changes in R-squared values is plotted for each of the three task parameters that were significant predictors in the GLM. **C:** Venn diagram illustrating the number of cue-modulated units encoding cue identity (blue circle), cue location (green circle), cue outcome (pink circle), as well as the overlap among units that encoded multiple cue features. **D:** Venn diagram illustrating the number of cue-modulated units encoding cue identity, cue location, and cue outcome during cue-onset (left circle), during nosepoke hold (right circle), and during both epochs (overlap). **E-G:** Sliding window GLM illustrating the proportion of cue-modulated units influenced by various predictors around time of cue-onset (E), nosepoke (F), and outcome (G). **E:** Sliding window GLM (bin size: 500 ms; step size: 100 ms) demonstrating the proportion of cue-modulated units where cue identity (blue solid line), cue location (red solid line), and cue outcome (yellow solid line) significantly contributed to the model at various time epochs relative to cue-onset. Dashed colored lines indicate the average of shuffling the firing rate order that went into the GLM 100 times. Points in between the two vertical dashed lines indicate bins where both pre- and post-cue-onset time periods were used in the GLM. **F:** Same as E, but for time epochs relative to nosepoke where the rat waited for the outcome. **G:** Same as E, but for time epochs relative to receipt of outcome after the rat got feedback about his approach. **H-J:** Average improvement to model fit. **H:** Average percent improvement to R-squared for units where cue identity, cue location, or cue outcome were significant contributors to the final model for time epochs relative to cue-onset. Shaded area around mean represents the standard error of the mean. **I:** Same as H, but for time epochs relative to nosepoke. **J:** Same H, but for time epochs relative to receipt of outcome.

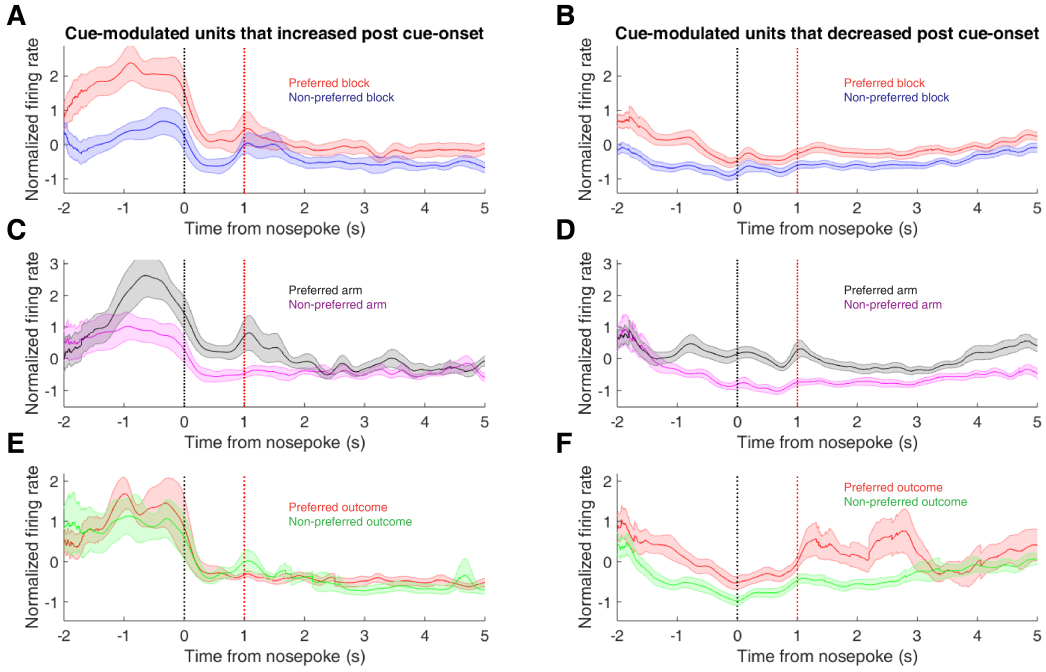


Figure 11: Population-level averages of cue feature sensitive NAc units during a nosepoke. **A:** Average smoothed normalized (z-score) activity for cue-modulated units where cue identity was a significant predictor in the GLM, aligned to nosepoke with reward delivery occurring 1 s after nosepoke. Activity is plotted for preferred stimulus block (red) and nonpreferred stimulus block (blue). Black vertical dashed line indicates nosepoke. Red vertical dashed line indicates reward delivery occurring 1 s after nosepoke for reward-available trials. Dashed color lines indicate the result of shuffling the identity of the units used for this average 1000 times. Lightly shaded area indicates standard error of the mean. Note larger increase leading up to nosepoke to preferred stimulus block over nonpreferred stimulus block. **B:** Same as A but for units that decreased in firing. Note the sustained difference in firing between the two blocks. **C-D:** Same as A-B for cue location. Activity is plotted for most preferred arm (black) and least preferred arm (magenta). **E-F:** Same as A-B for cue outcome. Activity is plotted for preferred expected outcome (red), and nonpreferred outcome (green). Note the peak after outcome receipt for preferred outcome in decreasing units (F).

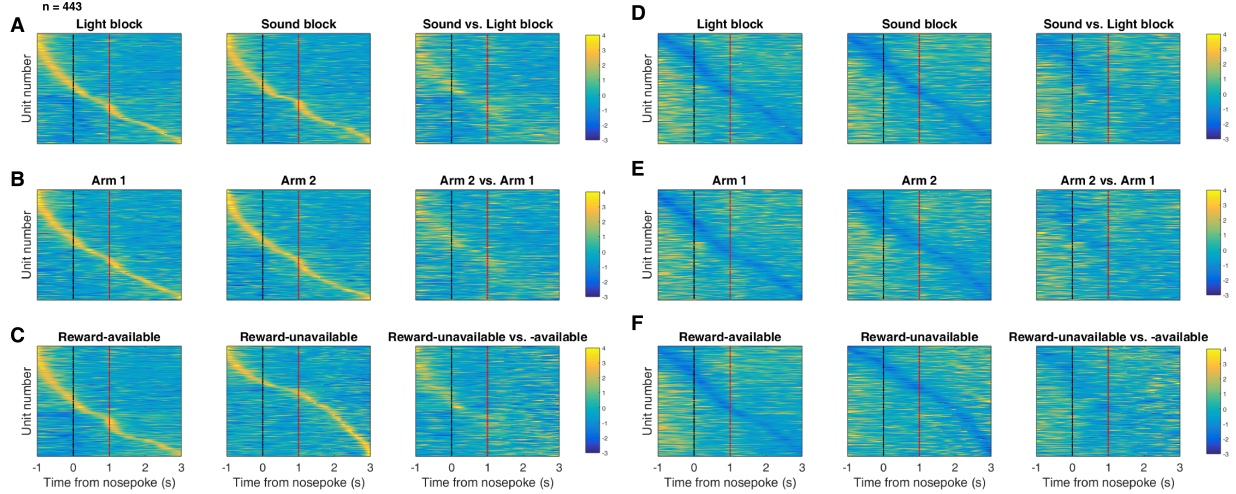


Figure 12: Distribution of NAc firing rates across time surrounding nosepoke for approach trials. Each panel shows normalized (z-score) firing rates for all recorded NAc units (each row corresponds to one unit) as a function of time (time 0 indicates nosepoke), averaged across all approach trials for a specific cue type, indicated by text labels. **A-C:** Heat plots aligned to normalized peak firing rates. **A, far left:** Heat plot showing smoothed normalized firing activity of all recorded NAc units ordered according to the time of their peak firing rate during the light block. Each row is a units average activity across time to the light block. Black dashed line indicates nosepoke. Red dashed line indicates reward delivery occurring 1 s after nosepoke for reward-available trials. Notice the yellow band across time, indicating all aspects of visualized task space were captured by the peak firing rates of various units. **A, middle:** Same units ordered according to the time of the peak firing rate during the sound block. Note that for both blocks, units tile time approximately uniformly with a clear diagonal of elevated firing rates, and a clustering around outcome receipt. **A, right:** Unit firing rates taken from the sound block, ordered according to peak firing rate taken from the light block. Note that a weaker but still discernible diagonal persists, indicating partial similarity between firing rates in the two blocks. A similar pattern exists for within-block comparisons suggesting that reordering any two sets of trials produces this partial similarity, however correlations within blocks are more similar than correlations across blocks (see text). **B:** Same layout as in A, except that the panels now compare two different locations on the track instead of two cue modalities. As for the different cue modalities, NAc units clearly discriminate between locations, but also maintain some similarity across locations, as evident from the visible diagonal in the right panel. Two example locations were used for display purposes; other location pairs showed a similar pattern. **C:** Same layout as in A, except that panels now compare correct reward-available and incorrect reward-unavailable trials. The disproportionate tiling around outcome receipt for reward-available, but not reward-unavailable trials suggests encoding of reward receipt by NAc units. **D-F:** Heat plots aligned to normalized minimum firing rates. **D:** Responses during different stimulus blocks as in A, but with units ordered according to the time of their minimum firing rate. **E:** Responses during trials on different arms as in B, but with units ordered by their minimum firing rate. **F:** Responses during cues signalling different outcomes as in C, but with units ordered by their minimum firing rate. Overall, NAc units "tiled" experience on the task, as opposed to being confined to specific task events only. Units from all sessions and animals were pooled for this analysis.

Task parameter	Total	\uparrow MSN	\downarrow MSN	\uparrow FSI	\downarrow FSI
All units	443	155	216	27	45
<i>Rat ID</i>					
R053	145	51	79	4	11
R056	70	12	13	17	28
R057	136	55	75	3	3
R060	92	37	49	3	3
Analyzed units	344	117	175	18	34
Cue modulated units	133	24	85	6	18
<i>GLM aligned to cue-onset</i>					
Cue identity	37	7	21	1	8
Cue location	50	13	27	3	7
Cue outcome	34	10	18	0	6
Approach behavior	31	8	18	1	4
Trial length	25	5	18	0	2
Trial number	32	11	12	1	8
Previous trial	5	0	5	0	0
<i>GLM aligned to nosepoke</i>					
Cue identity	66	14	36	2	14
Cue location	66	14	40	3	9
Cue outcome	42	8	29	0	5
<i>GLM aligned to outcome</i>					
Cue outcome	10	0	6	0	4

Table 1: Units overview